

Review

Additive Manufacturing of Bioinspired Structural-Color Materials

Zhilong Cao¹, Yanzhao Yang^{1,*}, Yuanhao Chen¹, Wei Feng^{1,*}, and Ling Wang^{1,2,*}

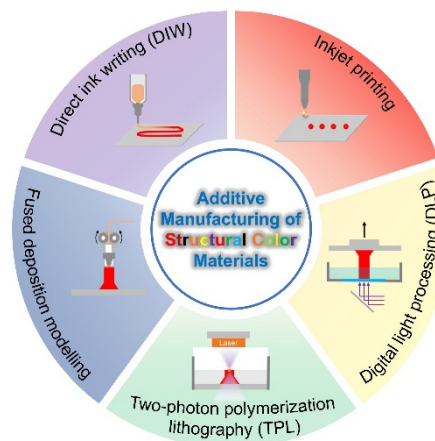
¹ School of Materials Science and Engineering, Tianjin University, Tianjin 300350, China

² Binhai Industrial Research Institute, Tianjin University, Tianjin 300452, China

* Correspondence: yangyanzhao@tju.edu.cn (Y.Y.); weifeng@tju.edu.cn (W.F.); lwang17@tju.edu.cn (L.W.)

Received: 8 January 2025; Revised: 2 April 2025; Accepted: 6 April 2025; Published: 19 May 2025

Abstract: Structural color is ubiquitous in nature and biological systems, and synthetic structural-color materials have been considered as a more durable substitute for traditional pigments. Recent advancements in the additive manufacturing of exquisite photonic objects have enabled the preparation of structurally colored materials with customized properties. Herein, an up-to-date review about additive manufacturing of bioinspired structural-color materials is presented. This review begins with an overview of the direct ink writing of colloidal crystals, chiral liquid crystals, cellulose nanocrystals, and block copolymers. Then, significant advances in inkjet printing strategy are showcased, including inkjet printing of colloidal crystals and cellulose nanocrystals, inkjet printing on photonic polymer coatings, and inkjet printing based on total internal reflections. The third section focuses on the recent advances in other additive manufacturing methods, including digital light processing, two-photon lithography, and fused deposition modeling. This review summarizes a perspective on potential opportunities, challenges, and future prospects encountered by advanced printing technology and functional structural-color materials.



Keywords: additive manufacturing; structural color; direct ink writing; inkjet printing; colloidal crystals; chiral liquid crystals

1. Introduction

Structural-color materials possess periodic dielectric nanostructures that reflect light at visible wavelengths, exhibiting vivid colors [1–5]. Nature has evolved different types of periodic nanostructures over millions of years of evolution to develop structural colors that intensify or weaken the visibility of biological organisms for purposes of camouflage, communication, and predator warning [6–8]. For instance, chameleons may camouflage by changing their skin colors to blend them with the background colors [9]. The spectacular iridescent colors of certain insects, opals, butterflies, plants, and peacocks are created due to periodic nanostructures on their surfaces that reflect light in specific spectral ranges [10–14]. Inspired by nature, investigators have proposed synthetic periodic nanostructures which offer nonfading, tunable, nontoxic, and iridescent structural colors [15–17]. In recent decades, structural-color materials have attracted substantial attention because of their fundamental importance and technological applications. The exploitation of exquisite structural-color patterns capacitates the manufacture of customized color images that are crucial for several emerging applications like sensors [18], decoration [19], bioanalysis [20], displays [21], anticounterfeiting [22], and optical communication [23]. Furthermore, three-dimensional (3D) structural-color materials enable the manipulation of optical properties and light paths, such as amplitude regulation, phase, and polarization, and generate new or enhanced optical properties [24]. In this context, functional structural color patterns and 3D structural color objects have been developed based on diverse fabrication strategies, including swelling [25], stamping [26], regioselective etching [27], mask-assisted



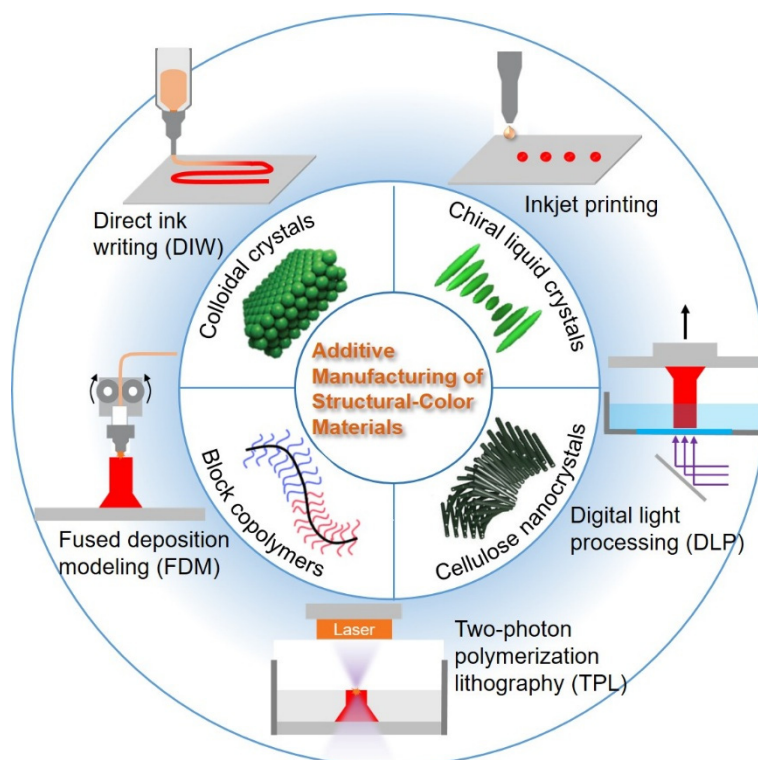
Copyright: © 2025 by the authors. This is an open access article under the terms and conditions of the Creative Commons Attribution (CC BY) license (<https://creativecommons.org/licenses/by/4.0/>).

Publisher's Note: Scilight stays neutral with regard to jurisdictional claims in published maps and institutional affiliations.

photography [28], and die making [29]. However, these methods require expensive tooling, lithographic masks, and time-consuming multi-step processes.

Additive manufacturing, which involves ink-based printing techniques that allow the digital design and manufacturing of exquisite patterns or 3D objects, is upgrading the science and engineering of advanced structural-color materials. In contrast to traditional manufacturing techniques, additive manufacturing enables the conversion of computer-aided designs into intricate objects as needed [30–36]. Additive manufacturing facilitates the on-demand production of customized products, characterized by specific shapes and sizes, while ensuring high production efficiency. This capability presents a significant economic actuation for its adoption across a range of industrial sectors, such as robotics, biomedicine, automotive, and aerospace [37–40]. Recently, additive manufacturing has emerged as a versatile method for fabricating structurally colored materials using micro- and nanoscale building blocks as printable inks. Several additive manufacturing approaches, including direct ink writing (DIW), inkjet printing, digital light processing (DLP), two-photon lithography (TPL), and fused deposition modeling (FDM), have been proposed for the manufacture of structural-color materials from diverse building block systems such as colloidal particles, chiral liquid crystals (CLCs), cellulose nanocrystals (CNCs), and block copolymers (BCPs). These printing platforms use building blocks in the following forms: polymer solution, photocurable resin, or thermoplastic monofilament. Additive manufacturing of structural-color materials currently stands in the limelight of research on account of the unparalleled advantages including remarkable universality, diversity, and stability. By carefully choosing the appropriate additive manufacturing parameters and techniques, it is possible to achieve sophisticated and customized patterns or 3D geometries of structural colors while attaining desirable optical properties.

Several reviews have focused on printable structural colors or the design of structural-color patterns [41–43]. To the best of our knowledge, there is no specific classification for the additive manufacturing of structural-color materials. Herein, an up-to-date account of the advancements in high-throughput printing methods capable of fabricating structural-color materials is showcased (Scheme 1). This review focuses on the following three aspects: In the first section, the DIW of colloidal crystals, CLCs, CNCs, and BCPs is introduced. The second section introduces recent significant progress in inkjet printing strategies, including inkjet printing of colloidal crystals, inkjet printing of CNCs, inkjet printing inks on photonic polymer coatings, and inkjet printing based upon total internal reflections. The third section summarizes the recent advances in other additive manufacturing methods, including DLP, TPL, and FDM. Finally, this review summarizes with perspectives on the opportunities and challenges in the future exploitation of additive manufacturing for structural-color materials.



Scheme 1. Schematic of additive manufacturing of structural-color materials. The additive manufacturing approaches include DIW, inkjet printing, DLP, TPL, and FDM. The building block systems used for printable inks include colloidal particles, CLCs, CNCs, and BCPs.

2. Bioinspired Structural-Color Materials and Additive Manufacturing Technologies

2.1. Principles of Bioinspired Structural-Color Materials

In nature, the brilliant iridescent colors of some opals, fruits, and butterflies are induced by the periodic nanostructures on their surface that reflect light in specific ranges of the spectrum. Taking lessons from nature, bioinspired structural color materials derive their colors from periodical micro-nanoscale structures that interact with light, which has been recommended as a more environmentally friendly and long-term stable alternative to traditional pigments and dyes. The photonic crystal structure is featured with long-range order. The characteristics of amorphous structure are short-range order. They all follow Bragg's law of light interference, diffraction, and reflection. These properties of structural colors hinge on the design of the structure-function relationship to a great degree [42].

According to the structural principles and fabrication techniques, structural-color materials can be categorized into colloidal crystals, chiral liquid crystals, cellulose nanocrystals, block copolymers, etc. As a few to name, opals have been known since ancient times (Figure 1a) [12]. The unusual gemstones are impressed by their gorgeous coloration that results from a highly ordered, densely packed arrangement of silica spheres with several microns in diameter indicated by scanning electron microscopy (SEM) (Figure 1b) [44]. Following suit, colloidal crystals can be formed by the self-assembly of monodisperse micro/nanoparticles in a facile and cost-effective manner like face-centered cubic packing, which possess long-range order to manipulate light and display vibrant colors with strong iridescence (Figure 1c). For practical coloration, it is essential to pattern colloidal arrays with a manipulated arrangement and robust mechanical stability in a reproducible and reliable way [45]. *Pollia condensate* is an African forest understory spherical species exhibiting bright metallic blue arising from Bragg reflection of helicoidally stacked cellulose microfibrils shown by transmission electron microscopy (TEM) (Figure 1d,e) [46]. CLCs have hierarchical architecture consisting of superimposing planar layers of parallel-aligned rod-like molecules/nanostructures with a certain twisting angle. This chiral morphology reflects circularly polarized light of the same handedness as the helicoid structure and transmits circularly polarized light with the opposite handedness (Figure 1f) [47]. The helical pitch of CLCs is proportional to the peak wavelength of the selective reflection. Thus, the reflection spectrum and the rendered structural color can be dynamically controlled via applying the physical stimuli to tune the helical pitch. The resulting helicoidal organization have been extensively studied to exploit structural colors which are iridescent, circularly polarized, tunable, and non-fading. Moreover, the inherent long-range order self-assembly of liquid crystals (LCs) can be a perfect characteristic for the manufacturing of structural-color materials on a large scale [48–50]. Especially, if LC molecular suffers a process of double-twist arrangement and self-organizes into a three dimensional (3D) periodic cubic lattices, blue-phase liquid crystals (BPLCs) are formed and treated as 3D photonic materials, whose name derives from the brilliant blue color when it was first discovered. [51–54]. BPLCs are widely utilized in flexible displays, tunable photonic devices, and biomimetic materials for the properties of the three-dimensional photonic bandgap and tunable structural coloration. CNCs are the crystalline regions of cellulose nanofibers, which consist of parallel linear cellulose chains bound by van der Waals forces and hydrogen bonding. The excellent amphiphilic character owing to different surface chemistries at varying crystal planes facilitates the heterogeneous interaction with other amphiphilic nanocomponents used in assembling hierarchical nanostructures similar to CLCs. The addition of water-soluble polymers can manipulate the mechanical stability and the pitch length of the chiral structures to fabricate brilliant structural-color patterns via evaporation-driven self-assembly [55]. *Morpho* butterflies' rainbow-like, shimmering iridescence can maintain bluish even over an extensive range of viewing angle, which is resulted from the light interference within the multilayered, periodic ridges on the scales covering the surface of their wings (Figure 1g,h) [56]. BCPs comprising a corporate backbone attached to grafted side chains are a promising substitute for linear block copolymers to fabricate the analogous one-dimension periodic structure and realize structural colors in the visible range [57]. The spatial repulsion among dense side chains generates more extensive cylindrical conformations and restrains chain entanglement, accelerating self-assembly into large ordered-region-size nanostructures (Figure 1i) [58]. The facile preparation of photonic crystals with BCPs holds promise for various potential applications containing the production of 3D-printed photonic structures, photonic pigments, photonic resins, and stress-responsive photonic structures [59,60]. In addition, woodpile photonic crystals (WPCs) as a specific structural-color material are fabricated through stacking plentiful parallel square columnar units in the vertical direction. The photonic band gaps of WPCs can be simultaneously and independently engineered in three dimensions to display structural colors with ultrahigh resolution due to the effective regulation of the nanometer-scale lattice constant, which are one of the most versatile platforms among the micro/nanodevices for the stability and scalability [61].

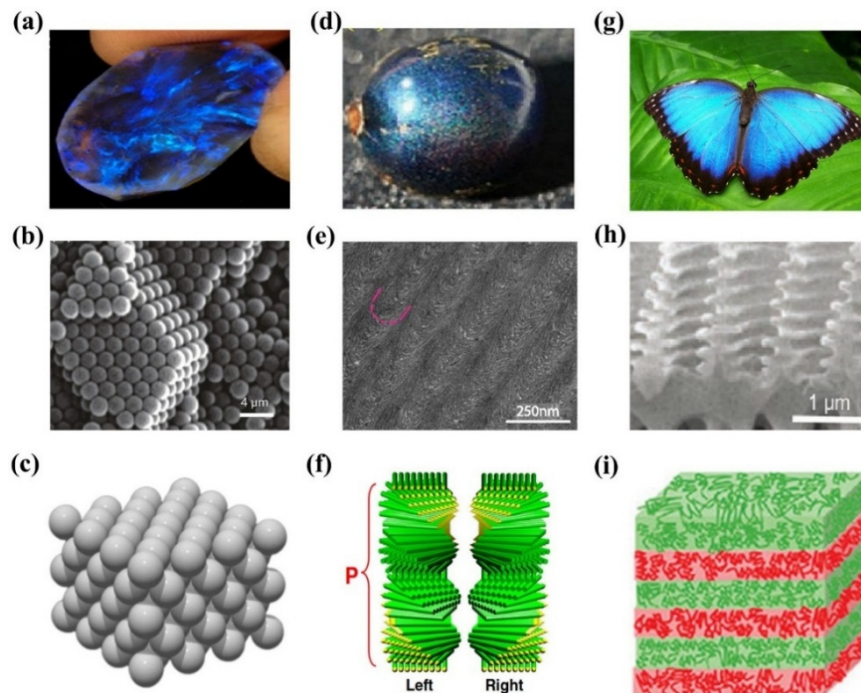


Figure 1. Photonic nanostructures in nature. (a) Photograph of black opal. Reproduced with permission [44]. Copyright 2011, Elsevier Ltd. (b) SEM image of the opal nanostructure. Reproduced with permission [12]. Copyright 2009, Wiley-VCH. (c) Schematic illustration of 3D self-assembly of colloidal crystals. (d,e) Photograph and TEM image of single *Pollia condensata* fruit collected in Ghana. Reproduced with permission [46]. Copyright 2012, National Academy of Sciences. (f) A schematic representation of the cholesteric helix for both handedness. Reproduced with permission [47]. Copyright 2014, Elsevier Ltd. (g,h) Photograph and cross-sectional SEM image of a *Morpho didius* butterfly. Reproduced with permission [56]. Copyright 2012, Wiley-VCH. (i) Schematic illustration of 1D BPCs prepared by hierarchical thermal self-assembly. Reproduced with permission [58]. Copyright 2020, American Chemical Society.

2.2. Additive Manufacturing Technologies

The remarkable advancement in additive manufacturing technologies has revolutionized the realm of the intelligent manufacturing system and offered remarkable universality, diversity, and stability for the preparation of structural-color materials. In accordance with the difference of logical sequence in operation, fabrication methods of additive manufacturing technologies for structural colors can be categorized into two types: top-down and bottom-up approaches. The former is to utilize multilayer deposition or lithography techniques to transform bulk materials into the desired micro-nano structures, such as DIW, inkjet printing and DLP. The latter relies on the self-assembly of basic building blocks through physical and chemical interactions to achieve ordered nanostructures, which includes TPL and FDM [62].

In DIW printing, nanoparticle clusters in liquid media with highly stable dispersibility and viscosity, which serves as the ink, are extruded directly onto a substrate for manufacturing materials with designed architectures and components, while a computer-controlled translation stage simultaneously moves the nozzle to realize an automated injection molding process [63]. Similar to DIW, inkjet printing has been more previously but commonly utilized in the patterned printing of structural-color materials. In inkjet printing, inks are ejected from a micrometer-sized printing nozzle as droplets and subsequently deposited onto the target substrates [64]. For DLP, particles dispersing in precursor solution polymerize under the irradiation of projected light to create a customized structure. A DLP machine can project 2D images sliced from target 3D objects, and the exposed parts are selectively polymerized. Once a layer was cured, the platform moved vertically for a certain distance and project the next image. Until the entire 3D object was constructed, this process needed repeat layer by layer [65]. In TPL processing, bulk materials produce localized photochemical reactions by utilizing high-energy pulsed lasers [66]. This technique enables the precise orientation and manipulation of chemical reactions in stereoscopic space, realizing the construction of high-precision structures on the micro-nano scale with a high-resolution [67]. Thermoplastic ingredients incorporated suitable building blocks can be melted into filamentous individuals and stacked layer-by-layer via FDM. These wires are self-assembled rapidly during the extrusion at high temperature. Desired products with centimeter-size 3D geometric shapes can be printed quickly and conveniently through this

process [68,69]. The selection of additive manufacturing technologies plays a pivotal role in determining the scalability, speed, and resolution of the process, meanwhile the choice of materials significantly influences the resulting color, durability, and performance of the structures. Thus, the properties of printable structural colors heavily hinge on the precision of structure construction fabricated by the printing technique employed and the options of materials.

3. Direct Ink Writing of Structural-Color Materials

For DIW of structural-color materials, the ink must be formulated for microscopic self-assembly properties and macroscopic printing rheology [70]. During the DIW printing, the parameters (e.g., the printing speed, pressure, and substrate temperature) could also make influences on the result of deposition and further control the quality of colors.

3.1. Direct Ink Writing of Colloidal Crystals

The DIW of colloidal crystals can be used to print photonic patterns according to the type of target substrate, color combination, and design. Colloidal crystal inks must be designed to provide a satisfactory printing rheology and conspicuous coloration after deposition.

Kim et al. reported the use of DIW with colloidal photonic inks in the preparation of customizable structural color graphics (Figure 2a) [71]. To eliminate the prolonged evaporation process, colloidal particles were designed with an exclusive interparticle potential lacking volatile components that induced particles to order spontaneously (Figure 2b,c). The lines were written directly through a dispenser using these inks, and the line width could be regulated by controlling the speed of writing. Faces were obtained through merging lines. The colloidal arrangement within the lines and the faces was scheduled to construct an amorphous array for relatively matte coloration or a crystalline array for strongly iridescent coloration in accordance with the viscosity of resins (Figure 2d,e). In addition, the structural-color patterns could be detached from the substrates for forming free-standing films or transferred onto other surfaces. Later, Kim et al. prepared elastic photonic microbeads via variable-size bulk emulsification and formulated photonic inks including microbeads for DIW [72]. The photonic inks retained the excellent color saturation of microbeads and provided reinforced capacity of printing. These printed graphics exhibited robust mechanical durability because of the elastic microbeads imbedded into the polyurethane matrix. Additionally, the resultant colors showed an extensive viewing angle with weak angle dependency by reason of light refraction at the interface of the air matrix and the optical isotropy of the single microbead. Color graphics can be determined by customers and printed on apparel and accessories for fashions. Besides, twinkling and iridescent colors and unique shape of the reflectance spectrum featured by a sharp single peak enable to function as anticounterfeiting patterns for top-secret documents and art masterpieces.

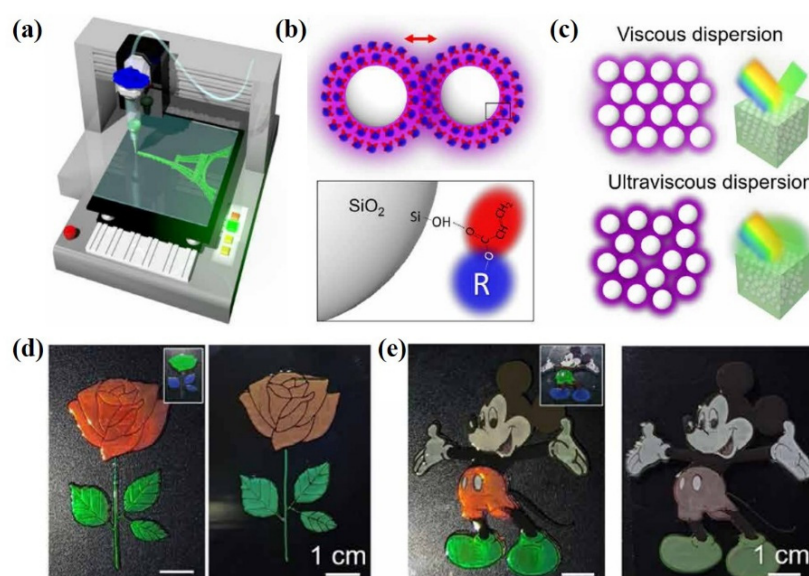


Figure 2. DIW of colloidal crystals. (a) Scheme of DIW of colloidal crystals. (b) Construction of a solvation layer on the silica surface with hydrogen bond assistance. (c) Crystalline and glassy packing in viscous ethoxylate acrylate (EA) and ultra-viscous urethane acrylate (UA). (d) Pattern of a rose and leaves printed directly with UA and EA inks. (e) Mickey Mouse written with UA and EA inks. Reproduced with permission [71]. Copyright 2021, AAAS.

3.2. Direct Ink Writing of Chiral Liquid Crystals (CLCs)

Currently, the fabrication techniques for CLC-based materials are often complicated owing to the inevitable employment of alignment procedures for uniform LC orientation and high-quality structural colors. Particularly for DIW, CLC inks must be formulated with satisfactory printing rheology for DIW [73–75].

In 2021, Sol et al. synthesized a CLC oligomer ink for DIW (Figure 3a) [76]. The ink was squeezed out of the nozzle and organized into a visually impactful cholesteric arrangement via a shear-induced alignment. Controlling the speed and writing direction generated a programmed construction of cholesteric liquid crystal elastomers (CLCEs) that exhibited polarization selectivity and atypical iridescence. This chiroptical photonic ink paves the way for design of specialized polymeric optical elements with disparate optical effects. The attractive and uniquely iridescent appearance of materials can be utilized in high-end decorative elements. Later, they synthesized a humidity-sensitive CLC oligomer ink for printing hydrochromic coatings that could be activated with aqueous hydrochloric acid solvent, inducing an obvious redshift in the reflectance spectrum when exposed to water (Figure 3b,c) [77]. No apparent negative impact had happened on the optical qualities of the material during the extended exposure to the acidic environment even up to 17 weeks, while resulting in swelling and changes in the reflectance spectrum due to the protonation. This stimuli-responsive ink can be integrated with information technologies and function as 3D-printed optical sensors and actuators.

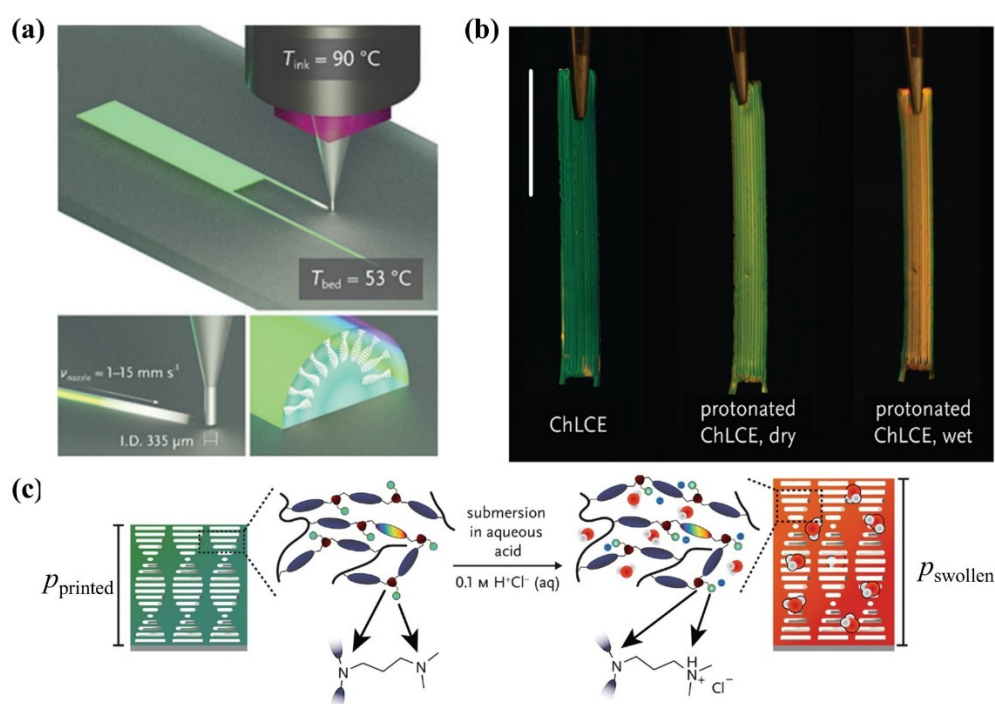


Figure 3. DIW of CLC oligomer inks. (a) Schematic of the DIW of the cholesteric liquid crystal elastomers (CLCEs) (top), mesophase transitions of the CLCEs (bottom-left), and the eventually proposed molecular structure for a perfect planar aligned CLCE (bottom-right). Reproduced with permission [76]. Copyright 2021, Wiley-VCH. (b) Free-standing CLCE films presenting visible color changes after protonating and pursuant exposure to water. Scale bar: 1 cm. (c) Schematic of the transition of CLCE undergoing acidic treatment, highlighting the occurrence of chemical modification with the synchronous change in the length of the cholesteric pitch. Reproduced with permission [77]. Copyright 2022, Wiley-VCH.

To create spatially controlled CLCE geometries, Choi et al. proposed DIW for CLCEs with a programmable mechanochromic response [78]. After deposition, the helical axis was tilted by approximately 32° relative to the printing direction for the combined effects of shear-induced alignment and the generated elongational force upon deposition onto the substrate. The printed CLC elastomers exhibited anisotropic mechanochromism when stretching owing to stretching-direction-dependent differences in the slant angle of the helical axis.

Because CLC oligomer inks are viscous, it is challenging to prepare well-defined helical nanostructures with outstanding color reflection [79–86]. The DIW of solution-processable and low-viscosity CLC inks for dynamic molecular self-assembly allows the preparation of structural-color graphics with vivid colors. Recently, our research group proposed solution-processable CLC inks for DIW of chiral structural-color patterns characterized

by bright colors and mechanochromic responses (Figure 4a) [87]. The solution-processable CLC inks were formulated optimally to enable microscopic self-assembly and macroscopic printing. After deposition onto target surfaces in line with preprogrammed trajectories, the monomers in CLC inks quickly self-organize into helical nanostructures through the evaporation-induced self-assembly process, in which Michael addition reaction enables to proceed in situ on the substrate for several hours at room temperature. The printed LCs are consequently polymerized by UV light for approximately 10 min to cure the microscopic helical arrangement. Multicolored, circularly polarized photonic patterns were fabricated on diverse substrates (Figure 4b). A concept of the circular-polarization cinefilm was proved by printing CLC inks which possess inverse chirality (Figure 4c,d). In addition, mechanochromic, circularly polarized photonic graphics were fabricated by printing CLC inks directly onto highly stretchable elastomeric films (Figure 4e). The as-proposed CLC inks were further printed on a wireless somatosensory electronic glove that can output synchronous visual and electrical signals. Upon bending the human fingers, the glove fingers accordingly stretch, resulting in immediate and simultaneous changes in the structural color and capacitance which can be converted into distinctive electrical signals. The interactively stretchable electronics possessing brilliant colors and antifading characteristics can be extensively utilized in numerous applications like entertainment, home healthcare, medical industry, and robotic control.

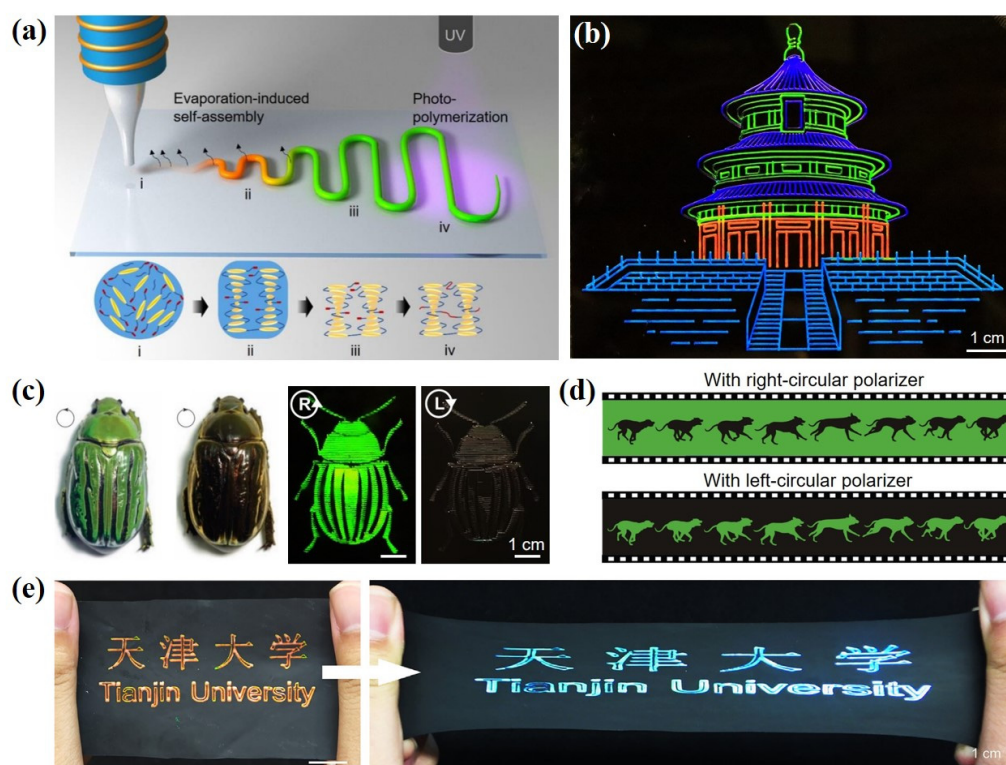


Figure 4. DIW of CLC molecular inks. (a) Schematic of DIW of CLC inks on glasses. (b) Temple of Heaven pattern printed by utilizing four kinds of CLC inks. (c) Beetle *C. gloriosa* (left) and the printed beetle patterns (right). Green iridescent color was observed with a right-circular polarizer and disappeared with a left-circular polarizer. (d) Circular polarization cinefilm via observation under right-circular polarizer (top) and left-circular polarizer (bottom). (e) CLC pattern changed colors from red to blue upon stretching. Reproduced with permission [87]. Copyright 2024, Elsevier Ltd.

3.3. Direct Ink Writing of Cellulose Nanocrystals (CNCs)

The range of wavelengths reflected by the CNCs films can be extended via introducing additives like polyethylene glycol (PEG) or hydroxypropyl cellulose (HPC) to enlarge the length of the cholesteric pitch. Cellulose-based materials can form photonic nanostructures and provide an opportunity to develop eco-friendly structural-color materials and coatings. HPC is an inexpensive, biocompatible cellulose capable of exhibiting lyotropic LC properties. At low concentrations (<40 wt.%), HPC aqueous solutions exhibit a disordered, isotropic structure and are extensively applied as thickening agents and binders in the food and pharmaceutical industries. At high concentrations (50–70 wt.%), polymer chains in a photonic chiral nematic phase constructed using HPC solutions self-assembled into helicoidal nanostructures similar to those found in scarab beetles.

Zhang et al. proposed a CNC ink for fabricating 3D structural-colored objects (Figure 5a) [88]. Two other elements, poly(acrylamide-co-acrylic acid) (PACA) and gelatin, were incorporated into the HPC solutions to produce printable HPC-gelatin-PACA ink. PACA could maintain the shape after printing by in-situ UV crosslinking, and gelatin afforded appropriate rheological properties during printing. This ink can be designed into 3D customized objects on substrates to exhibit angle-independent and vivid structural colors (Figure 5b–d). The resultant macroscopic 3D objects exhibited color adjustability under the control of the ambient temperature owing to the synergic thermoresponsiveness of PACA and HPC. Thus, this CNC ink system can be extended to daily-life commodities including colorant-free decorations in wearable biosensors, cosmetics, and drugs, as well as food industry or customized bionic skins.

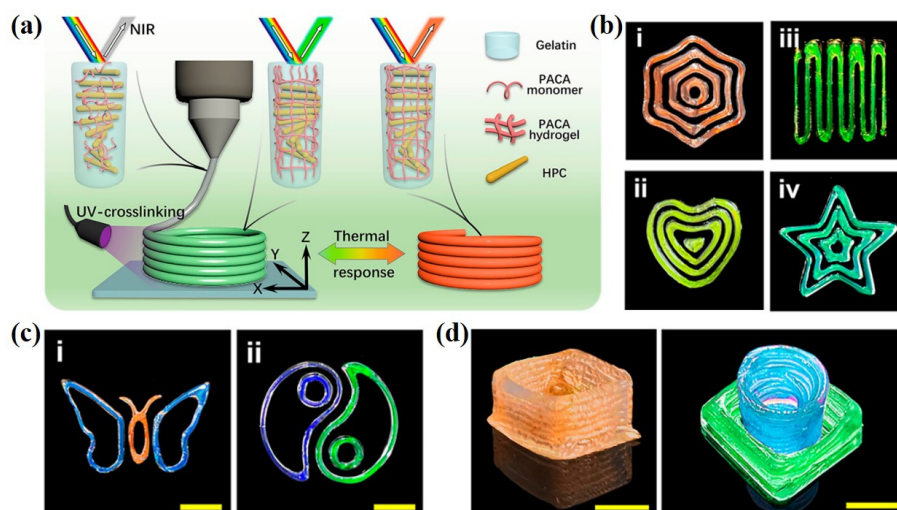


Figure 5. DIW of CNCs. (a) DIW of CNC inks for 3D structural coloration. (b) Single-colored graphics. (c) Multicolored graphics. (d) 3D objects. Scale bars: 4 mm. Reproduced with permission [88]. Copyright 2022, National Academy of Sciences.

Similarly, George et al. incorporated PEG into anisotropic HPC solutions to establish printable CNC inks for the DIW of CNCs [89]. At higher shearing rates (97 s^{-1}), the alignment along print paths at an approximately 20° could be attained, generating the coloration with high angle dependence. Materials with unique chiroptical properties displaying an optical response to mechanical deformation were fabricated due to the plasticizing effect of PEG in conjunction high-shear-rate extrusion. The utilization of path-dependent cholesteric domains to be an additional parameter expanded the design space further and allowed the response pattern to be modified by changing the infilling path of objects. The aesthetics of the materials acquired by HPC-based inks during high- or low-shear extrusion afford a sustainable source of structural colors capable of being utilized in optical sensing and coating applications.

Despite the capability of DIW to accomplish the printing of some complex-shaped 3D structural-colored materials, it is limited by inherent defects, leading to pervasive challenges such as coarse surface texture, constraints in material versatility, and reduced printing precision. In DIW, the ink is extruded through a nozzle, which means that the printing resolution is limited by the nozzle diameter. In addition, to achieve a bright structural color, a lengthy post-treatment is necessary, which may cause material cracking. These limitations restrict the application of DIW in printing high-precision structural-colored materials.

3.4. Direct Ink Writing of Block Copolymers (BCPs)

For high-production volume printing of BCPs, Patel et al. reported customizable DIW for BCP deposition to achieve functional, spatial, and microstructural patterning of structural colors (Figure 6a) [90]. Well-designed poly(dimethylsiloxane)-block-poly(lactic acid) (PDMS-b-PLA) bottlebrush BCPs were used as ink. The structural colors of bottlebrush photonic crystals could be modulated via controlling the bed temperature and printing speed during DIW printing (Figure 6b). After the comparison of printed samples, a pronounced blueshift in reflected wavelength is observed as printing speed increases, while increasing temperature results in a marked redshift. The intricate spatial and functional control for depositing more versatile patterns like the chameleon pattern comprising diverse colors printed as sequential layers via nonequilibrium assembly techniques with the integration of hardware and software approach.

Jeon et al. achieved the dynamic tunability of structural colors during printing by integrating polystyrene-block-poly(lactide) (PS-b-PLA) cross-linkable BCPs with a UV-supported 3D printer (Figure 6c) [91]. By employing a single ink material, multiple colors were achieved within a single printing process by UV-crosslinking-driven kinetic trapping of the evaporative assembly. The technique realized the preparation of structural colors from dark blue (392 nm) to orange (582 nm) in the visible wavelength spectrum through reducing UV light irradiance from 411 to 0 $\mu\text{W}/\text{cm}^2$. A mimic of Van Gogh’s “The Starry Night” with yellow-to-green-to-blue village, yellow-to-green moonlight, and blue-to-green night sky through programming the temporal profile of UV light irradiance to create patterns with color gradients merely adopting a single ink material. (Figure 5d). It can be predicted that this approach would shine light on anticounterfeiting patterns for art masterpieces and decorations in luxurious furniture.

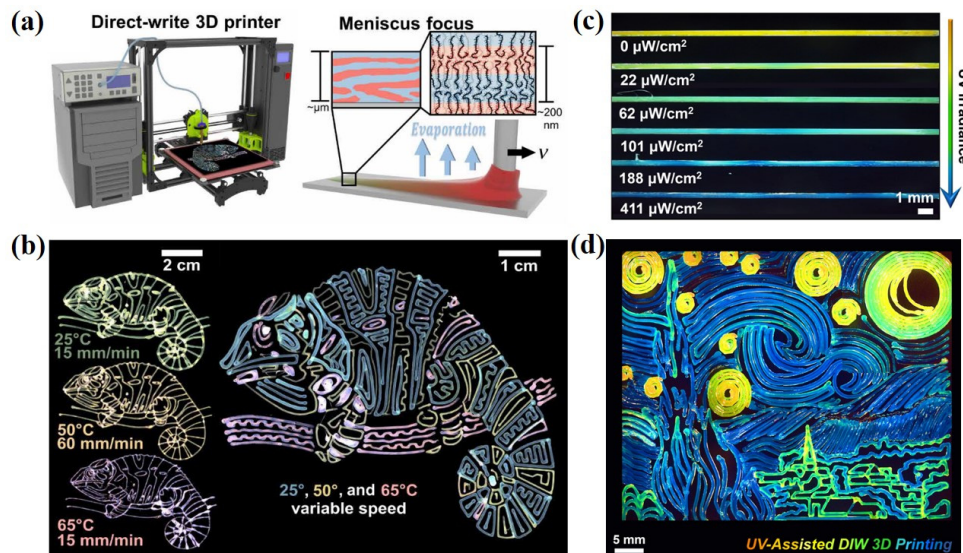


Figure 6. DIW of BCPs. (a) Scheme of molecular self-assembly and DIW of BCPs during the solution-casting process. (b) Chameleon patterns created under stationary printing conditions (bed temperature, pressure, and printing speed) as successive prints. Reproduced with permission [90]. Copyright 2020, AAAS. (c) Printed lines under various standards of irradiance of UV light when printing. (d) Starry Night pattern fabricated via dynamic UV-assisted DIW printing. Reproduced with permission [91]. Copyright 2024, National Academy of Sciences.

4. Inkjet Printing of Structural-Color Materials

Inkjet-printed structural-color materials could be categorized into two types according to the mechanism of generation of structural-color patterns: drop-on-demand inkjet-printed inks on substrates and continuous inkjet-printed inks on photonic polymer films. In drop-on-demand inkjet printing, droplets are merely created and ejected when needed, allowing for minimal material usage, smaller drop size generation, higher placement accuracy, and low cost. Typically, drop-on-demand inkjet printing is a functional technique for preparing structural-color patterns by integrating direct writing with particle self-assembly in droplets [92–94]. The inkjet-printing quality of structural-color patterns is subject to elements such as ambient temperature, humidity, substrate wettability, ink composition, and inkjet printing parameter settings. Continuous inkjet printing of inks on photonic polymer films is an emerging strategy for printing multicolor patterns [95,96]. The advantage of this strategy is that the pattern can be erased by removing the ink and reprinting.

4.1. Inkjet Printing of Colloidal Crystals

Song et al. achieved significant results and made tremendous contributions to the preparation of patterned colloidal crystals for practical applications [97–99]. In their researches, structural-color patterns containing dots, lines, and surface shapes were fabricated successfully by the self-assembly of colloidal nanoparticles via adjusting the preparation conditions of inkjet printing. For the dot-like structural-color patterns, inkjet printing was applied to deposit latex droplets onto an octadecyltrichlorosilane-treated substrate which afforded a high receding contact angle and enabled free sliding of the three-phase contact line (TCL). All the particles within each droplet were driven inwardly during the drying process for the effect of the free-sliding TCL and assembled into structural-color domes spontaneously, realizing a great height-to-diameter (H/D) ratio (Figure 7a) [100]. The printed structural-color domes had a uniform shape and size with the particles assembled into a densely-packed face-

centered cubic structure. Interestingly, structural-color domes with H/D ratios exceeding 3/8 exhibited angle independence (Figure 7b). This convenient printing approach affords an efficient method for exploiting displays with extensive viewing angles. The facile printing approach could offer a high-efficiency strategy for creating advanced displays and other optical devices. DIW-printed advanced displays based on structural-color materials through this method can control the phase, amplitude, and polarization of light at subwavelength scales as beam deflectors and optical encryption devices. Structural-color optical sensors capable of making adjustment to their reflection wavelength in response to environmental stimuli can be extensively applied in environmental monitoring, biosensing, and wearable health diagnostics.

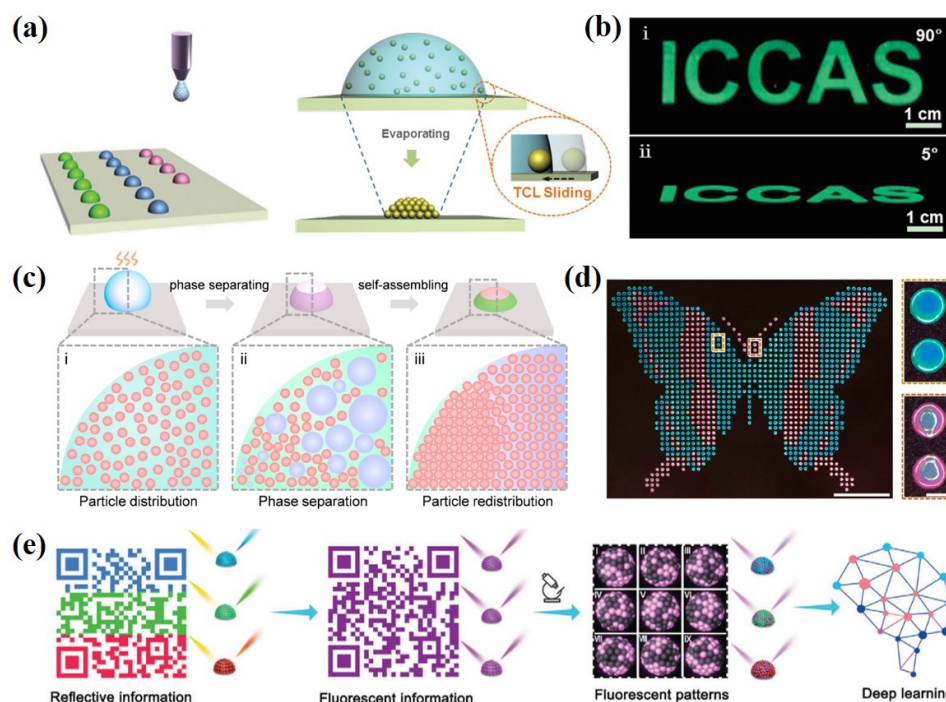


Figure 7. Inkjet printing of colloidal crystals. (a) Inkjet printing patterned PC domes onto hydrophobic surfaces through adjusting the sliding TCL. (b) Fluorescent structural-color domes' angle-independence of the fluorescence images. Reproduced with permission [100]. Copyright 2014, Wiley-VCH. (c) Schematic of the fabrication of dual-color domes on a basis of phase separation. Reproduced with permission [101]. Copyright 2022, American Chemical Society. (d) A butterfly-like pattern printed via heterogeneously self-assembling on a PDMS substrate. 180 nm and 220 nm silica nanoparticles were utilized to construct green-blue and red-green depositions, respectively. Scale bar: 1 cm; zoom in 0.5 mm. Reproduced with permission [102]. Copyright 2023, American Chemical Society. (e) Inkjet-printed pattern combined with the structural colors and fluorescence for multiplex encryption and anticounterfeiting. Reproduced with permission [103]. Copyright 2024, Wiley-VCH.

Dual-color spots are significant identity labels that deliver warnings and mating information. Li et al. developed a one-pot method on a basis of the phase-separation-associated non-uniform self-assembly of silica nanoparticles to fabricate dual structural-color domes (Figure 7c) [101]. In the drying droplets, individual nanoparticles were nonuniformly distributed into two compartments owing to the varying compatibility of nanoparticles between the two phases and the droplet inner flows. The colors of the domes resulted from nanoparticles' self-assembly are capable of being programmed via modulating the assembly conditions. A tremendous volume of content in encrypted patterns was designed using dual-color domes, presenting promising applications for information transfer. Later, Li et al. utilized the spatial restriction induced owing to the skin layer packaging of a drying colloid PEG droplet to enable the heterogeneous self-assembly of individual nanoparticles (Figure 7d) [102]. Colloidal crystals with homogeneous or heterogeneous plane orientations were fabricated by modulating the concentration of PEG within the droplets. This heterogeneous self-assembly approach enables the extensive utilization of various colloidal nanoparticles, different droplet shapes, and diverse substrates. Coatings fabricated by this strategy have the advantages of tunable colors, unfadeness, and low-energy consumption, which can be extensively used in anti-counterfeiting for economic security and human health.

The combination of fluorescence and structural color is a good strategy for fabricating multiplex encryption systems. Gao et al. proposed a robust multiple encryption system with integration of structural color and

fluorescence via programmable inkjet printing using colloidal photonic inks (Figure 7e) [103]. Colloidal photonic crystals exhibit structural-color patterns under sunlight. Under UV light, those exhibiting fluorescence in the same region display different fluorescence patterns. Microscopic fluorescence patterns which are unclonable physically can be observed in specific regions with fluorescence microscopy, the resulting macroscopic dual-mode encryption offered strong identifiable encrypted information. Moreover, evaporation process-induced fluorescence patterns exhibit unparalleled, uniform, and irrelevant random properties with high complexity and sufficient encoding capacity and further deep learning could be employed to construct a database and certify its credibility. It is expected that this system will provide a promising technique to combat counterfeiting and reinforce the practical application of fluorescent and structural colors for anticounterfeiting in high value products.

4.2. Inkjet Printing of Cellulose Nanocrystals (CNCs)

CNCs are ideal candidates for use as cost-effective and sustainable inks to print bespoke patterns and scalable photonic coatings. Whereas, the small volume and large surface area of sessile CNC droplets typically generate rapid evaporation, producing microfilms with a coffee-stain-like morphology and pretty vague coloration. Williams et al. proved that inkjet printing of CNC droplets directly via an immiscible oil layer enables instantly inhibit water loss, realizing a reduced internal mass flow and more sufficient time used for cholesteric self-assembly [104]. The color of individual microfilm depended on the initial composition of the droplet, which was capable of being adjusted as required through leveraging the overprinting and coalescence of numerous smaller droplets of various inks. The approach realizes the fabrication of multicolored patterns with intricate optical behaviors, like polarization-selective reflection and angle-dependent color. Finally, the array could be achieved responsive to stimulations (e.g., polar solvents and UV light) by the inclusion of degradable additives. These advantageous properties make inkjet-printed photonic CNC arrays suitable for optical anticounterfeiting and smart colorimetric labeling applications. It can be envisaged that high-quality, full-color photonic patterns could be highly compatible with the stringent processability demands of commercial printing including packaging labels.

4.3. Inkjet Printing Inks on Photonic Polymer Coatings

In 2018, Schenning and coworkers proposed inkjet printing of CLC inks on photonic polymer coatings for the first time (Figure 8a) [105]. They first prepared CLC polymer coatings containing nonpolymerizable LCs. Elimination of the non-polymerizable cyanobiphenyl LC derivative (5CB) resulted in the collapse of the polymer network, achieving to reduce the helical pitch length and impart a violet color to the coatings. This process also made the network highly flexible and optical response to stimuli enhanced. Moreover, this flexible network can be swollen using nematic-phase LC inks E7, which could be readily filled in an inkjet printer cartridge and precisely introduced at the desired areas in a controlled method. The wavelength of the reflected light is in direct proportion to the helical pitch length. Therefore, full-color images can be patterned on polymer coatings through inkjet printing with different amounts of LC ink on demand. Importantly, the printed patterns exhibited stability and durability under ambient conditions and could be entirely erased to allow for printing another new pattern. The fully rewritable and printable photonic coating from a CLC polymer network paves the avenue for rewritable photonic papers and arbitrary polymer patterns responsive to external stimulus.

For universal patterning of program dual-mode images, Liu et al. designed fluorescent LC polymer coatings to create geminate patterns using two-chromatic inkjet printing technique (Figure 8b) [106]. Nanocomposites as a novel paradigm of fluorescent LC materials integrate colloidal quantum dots with CLC polymer networks for producing extensive color palettes of photoluminescence and Bragg reflection. Based on two-chromatic inkjet printing technology, geminate, high-resolution, and full-color patterns with two colors of different mechanisms have been inkjet printed, for example, fluorescent dragon and reflective Phoenix.

BPLCs can be used as photonic polymer coatings for inkjet printing. Yang et al. fabricated a printable photonic polymer coating was on a basis of a monodomain BPLC network (Figure 8c) [107]. BPLC polymer coatings were covalently bonded to a glass substrate that was patterned with LC ink to swell the polymer network. The degree of swelling was determined by the amount of LC ink printed, which could be manipulated via regulating the voltage of the inkjet printer. Random multicolor patterns spanning the visible light wavelength from 451 to 618 nm could be printed and erased multiple times, rendering these BPLC polymer coatings shine light on responsive photonic materials and rewritable photonic papers. Meng et al. reported a high-resolution “live” pattern was resulted from the well-scheduled diffusion of LC ink on BPLC polymer networks with modified wettability (Figure 8d) [108]. This hydrophobic substrate significantly suppressed random spreading and diffusion of the ink, generating high-resolution patterns. BPLC materials featured with the intrinsic properties like ultrafast electro-

optical switching and wide viewing angle generate field-sequential color displays in the millisecond range, which function as advanced optical communication and adaptive photonic devices.

In addition to LC inks, water can also be used as an ink for inkjet printing. Yang et al. fabricated humidity-responsive, color-changing photonic polymer coatings on a basis of hydrogen-bonded BPLC networks [109]. The polymer coatings exhibited humidity-responsive reversible color changes in the visible spectrum of light, which were driven by breaking the hydrogen bonds and subsequently converted into hygroscopic polymer coatings. Rewritable photonic patterns were obtained by inkjet printing water onto the dried hygroscopic BPLC polymer coatings. This work shines light on applications in diverse civil and military fields containing adaptive camouflage, information encryption, sensors, and beyond.

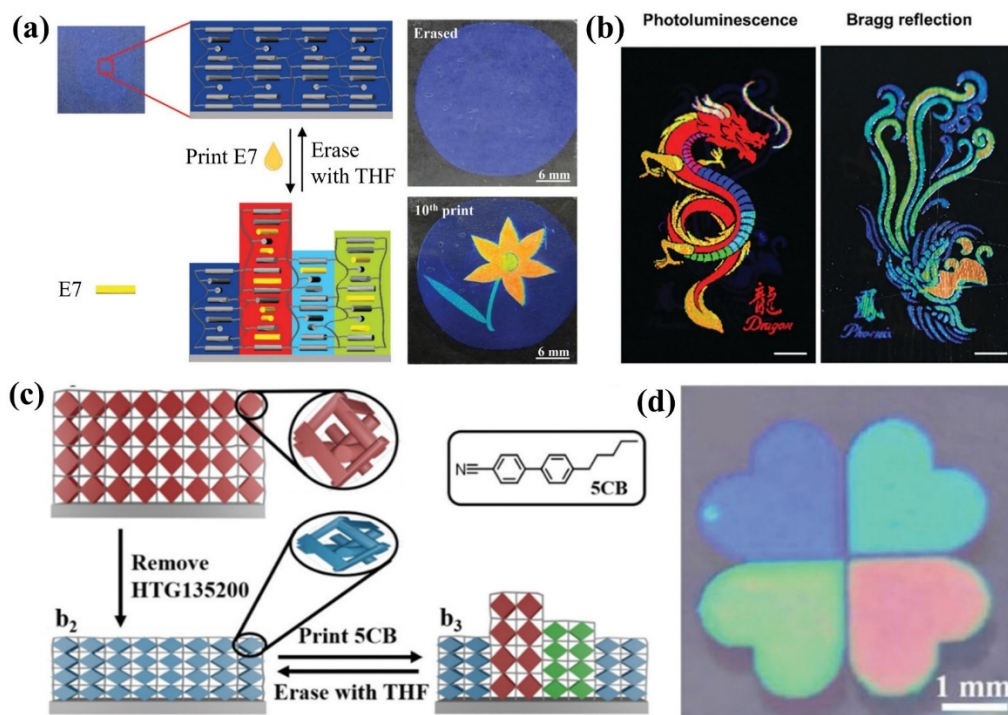


Figure 8. Inkjet printing of LCs on photonic polymer coatings. (a) Working mechanism of patterning in the CLC polymer coating. Reproduced with permission [105]. Copyright 2018, The Royal Society of Chemistry. (b) Photographs of a full-color pattern achieved by two-chromatic printing technique to display the images of fluorescent Dragon and reflective Phoenix upon UV excitation and white light irradiation, respectively. Scale bars: 5 mm. Reproduced with permission [106]. Copyright 2024, Wiley-VCH. (c) Working mechanism of patterning in the BPLC polymer coating. Reproduced with permission [107]. Copyright 2019, The Royal Society of Chemistry. (d) Four-leaf flower pattern created through well-designed multilayer printing on a BPLC polymer coating. Reproduced with permission [108]. Copyright 2022, Wiley-VCH.

4.4. Inkjet Printing Based on Total Internal Reflections

In 2020, Goodling and Zarzar illustrated brilliant structural colors could be created at microscale concave interfaces and proved the coloration principle of interference due to total internal reflections systematically, thereby establishing the feasibility of manipulating the structural colors using low-index materials [110]. The structural colors of total internal reflections could be directly achieved using single microstructure without applying complex particle self-assembly or polymer phase-separation structures [111–113].

Based on the total internal reflection effect, Li et al. developed a facile structural-color printing technique were capable of realizing the full-color fabrication of highly photorealistic images with an individual transparent ink by the commercial inkjet printing approach (Figure 9a) [114]. Transparent inks can be produced in a large quantity from monomer or polymer solutions. When ink droplets are printed on a transparent and hydrophobic substrate, they retract into the ideal microdomes with large curvature angles for the effect of surface tension. These inverted microdomes can generate an interference color from total internal reflections and function as independent pixels for constructing the color images. The color of each microdome which was controlled by the optical path is adjusted across the whole visible region by modulating the physical morphology (Figure 9b). Thus, we can facilely gain full-color pixels using one transparent ink and one printing nozzle. Every pixel was decoded into the

corresponding printing parameters, and a digital programmable printer was utilized to prepare the full-color structural-color images. The lightness, grayscale, gamut, and saturation of the image can be systematically manipulated using single-pixel precision (Figure 9c). Additionally, this color-printing approach is entirely compatible with the commercial printing technique and is suitable for large-scale industrial production. Therefore, it is greatly anticipated that the optical Janus property of coloration and transparency gained from different sides will facilitate structural colors for the practical applications in colorimetric sensor, anticounterfeiting technology, dynamic display, and smart window. For instance, the facile flipping can realize the fully reversible switching between radiative cooling and heating due to the asymmetrical optical effect.

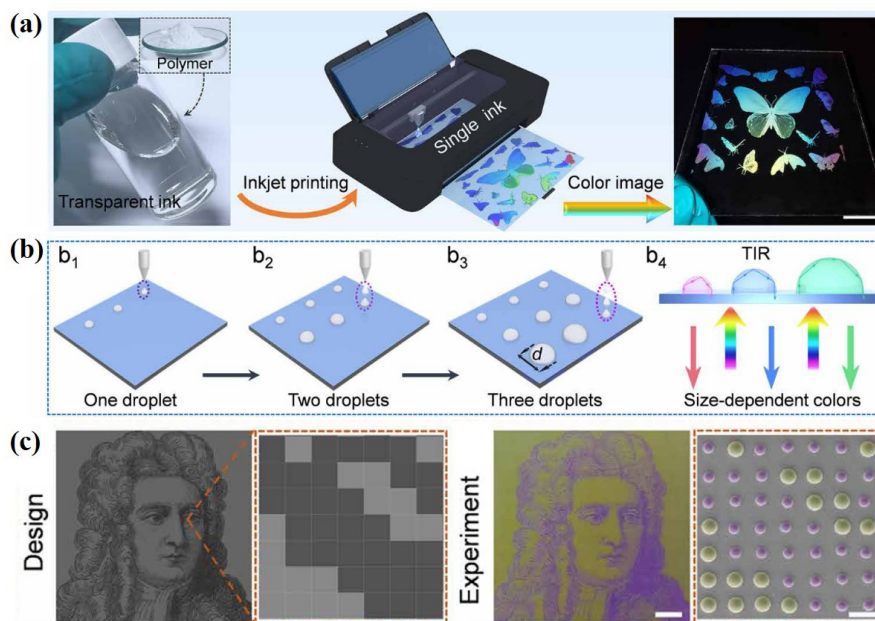


Figure 9. Full-color printing based on total internal reflections. (a) Process of structural-color printing with an individual transparent polymer ink. Polymer ink can be directly created by dissolving the polyacrylic acid into the mixture of ethylene glycol and water. Scale bar: 2 cm. (b) Schematic of the D-B-D printing (b_1 to b_3) to fabricate and integrate the different microdomes through which the microdome diameter can be controlled precisely. Viewing from the bare-glass (blank) side (b_4), the microdomes can display size-dependent colors for diverse optical paths of total internal reflection. (c) Designed grayscale and experimental colorful patterns of Isaac Newton's portrait. Scale bars: 40 μm . Reproduced with permission [114]. Copyright 2021, AAAS.

5. Other Additive Manufacturing Methods for Preparing Structural-Color Materials

5.1. Digital Light Processing (DLP)

The formulation of precursor solutions for DLP printing is critical for the successful printing of 3D structures with ideal performance. Specifically, the precursor solutions used in DLP printing consist of monomers, cross-linking agents, and photosensitizers, which can be cured by the phase transition from liquid to solid during exposure to UV or blue light. Because precursor solutions containing colloidal particles have been extensively utilized in the fabrication of patterned photonic crystal films, they can also be cured layer-by-layer to theoretically establish a 3D structure through integration with DLP [115]. DLP enables the fabrication of complex, high-resolution aesthetic patterns with durable structural colors. DLP-printed structural-color materials can be precisely engineered to manipulate light for sensing, display, and counterfeiting technologies [116].

Liao et al. were the first to report a combination of DLP and precursor solutions containing colloidal particles [117]. They reported a printable colloidal photonic crystal ink consisting of highly charged elastic nanoparticles (HENPs) achieved dispersion in a precursor solution. They fabricated 3D colloidal photonic crystal hydrogels with macroscopic geometries and the corresponding structural colors using DLP (Figure 10a,b). The key to this approach is to preserve the ordered arrangement of the HENPs in the precursor solution through electrostatic interactions before printing. During the printing process, the precursor solution polymerizes under the projected pattern, which locks the arrangement of the HENPs into the printed structure. Consequently, a 3D customized object with a stable structural color is formed. This approach allows the production of 3D colloidal photonic crystal hydrogels with the desired functions by tuning the ink composition or printing parameters. For

instance, using an ink containing a thermoresponsive monomer, such as N-isopropylacrylamide (PNIPAm), they prepared bioinspired structures that exhibit color variations corresponding to temperature changes. The tunable and reversible structural-color performance reinforces the practical applications like color-morphing soft robots for surveillance, reconnaissance, and wildlife observation without disturbing natural habitats.

However, the printing process in this method is non-continuous, as each consequent layer cannot be printed until the previous layer is complete. This limitation results in a layered structure with a rough surface and poor fidelity. To solve this problem, continuous DLP has been proposed, and a similar method has been successfully employed for the fabrication of structural-colored materials.

Zhang et al. utilized a hydrogen-bond-assisted colloidal resin to print 3D structural-colored materials which have been self-assembled well through a previously developed one-droplet 3D printing strategy (Figure 10c–f) [118]. During the printing process, the resin was refilled while the supporting platform was simultaneously elevated. Figure 9d,e shows the ink composition and the final printed structures. In the UV-curable system, polystyrene latex particles as the structural color provider, carbon black designed to decrease incoherent scattering, and photocurable monomers were stabilized by hydrogen bonds between them during printing. Meanwhile, using the continuous curing method, the pressure difference between the newly filled resin and the already cured layer creates a suction force that ensures the inward filling of the resin and tight self-assembly of the colloidal particles within the cured layer. Just-printed objects exhibit minimal structural colors. After the removal of water via evaporating, the printed objects can construct a densely arranged hexagonal colloidal particle structure to generate a brighter structural color. Moreover, the structural color could be fine-tuned through controlling the printing speed and particle diameter [119–123].

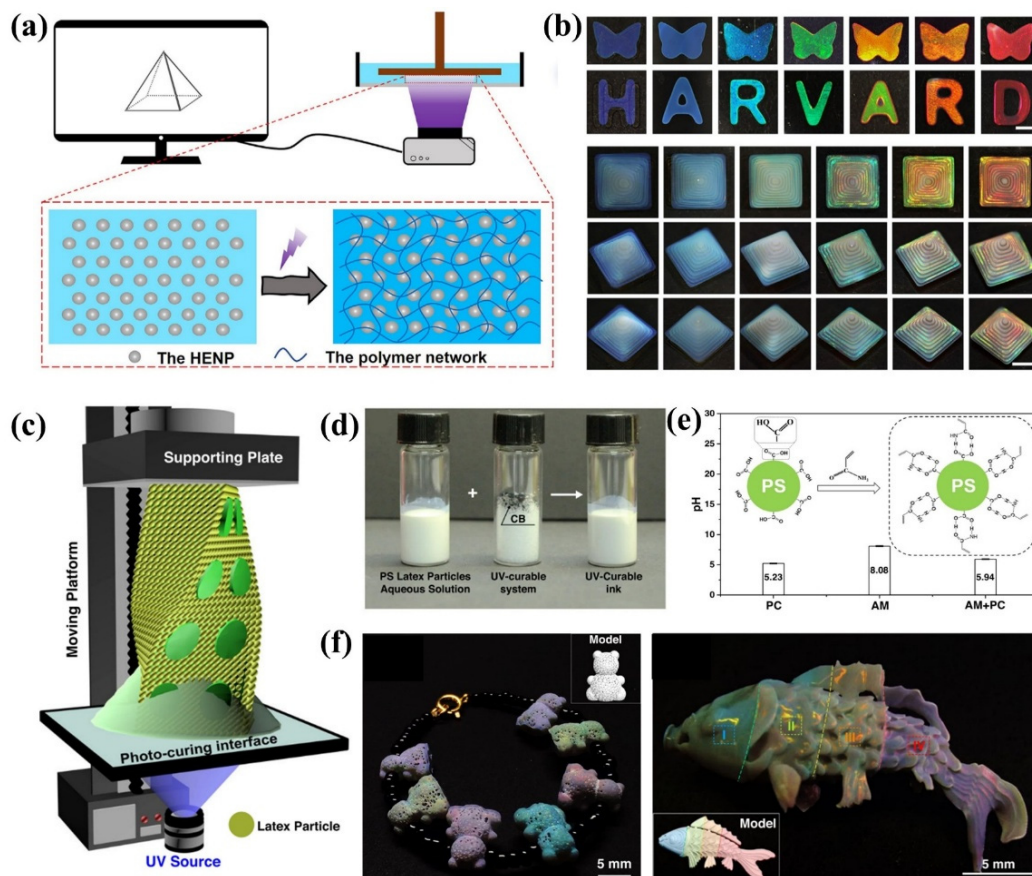


Figure 10. Structural-color materials via DLP. (a) Schematic of the DLP 3D printing of colloidal photonic crystals. (b) Printed 2D and 3D non-close-packed colloidal photonic crystals with different colors. Scale bars: 2 mm. Reproduced with permission [117]. Copyright 2024, Elsevier Ltd. (c) Scheme showing the process of consecutive resin refilling and hydrogen bond-assisted synergistically DLP 3D printing apparatus. (d) UV-curable structural-color ink formation. (e) pH characterization of pure aqueous dispersion solution of PS latex particles, pure aqueous solution of monomer acrylamide (AM), and aqueous mixture of PS latex particles with AM. (f) Optical images of the multiple structural-color models printed using various PS latex particle diameters. Reproduced with permission [118]. Copyright 2022, Nature Publishing Group.

5.2. Two-Photon Polymerization Lithography (TPL)

TPL relies primarily on a process known as two-photon polymerization. During this process, the photoinitiator at the laser focus simultaneously absorbs two photons and generates radicals that trigger polymerization in the photoresist. TPL has been extensively investigated for the manufacture of various 3D micro/nanodevices with high resolutions, which can be utilized in fluidic devices, optical materials, metamaterials, and cell cultures [124].

Using TPL technology, freely designed structural-color materials with highly ordered 3D nanostructures could be prepared using photoresists. However, creating forbidden gaps in the visible light wavelength desires a high resolution that exceeds that of the regular TPL system. The laser-writing process disturbs the stable microenvironment in the photoresist and results in unwanted polymerization within the surrounding regions. To overcome this challenge, Liu et al. proposed a heat-shrinking technique was leveraged to fabricate 3D-printed photonic crystals which possessed a $5\times$ reduction in the lattice constants, realizing sub-100-nm features with a full spectrum of colors (Figure 11a,b) [125]. The lattice structures as 3D color volumetric elements facilitated the printing of the 3D microscopic scale objects, such as the first multicolor microscopic model of the Eiffel Tower, which measured just 39 μm in height and a color pixel size of 1.45 μm . This method for printing colorful 3D structures at the microscopic scale offers significant potential for direct patterning and the integration of spectrally selective devices, including photonic crystal-based color filters, onto curved surfaces and freeform optical elements. This ability to precisely produce structural color within complex 3D objects could be extended to developments in integrated 3D photonic circuitry and compact optical components, achieving position tracking and full-color wide angle panoramic views.

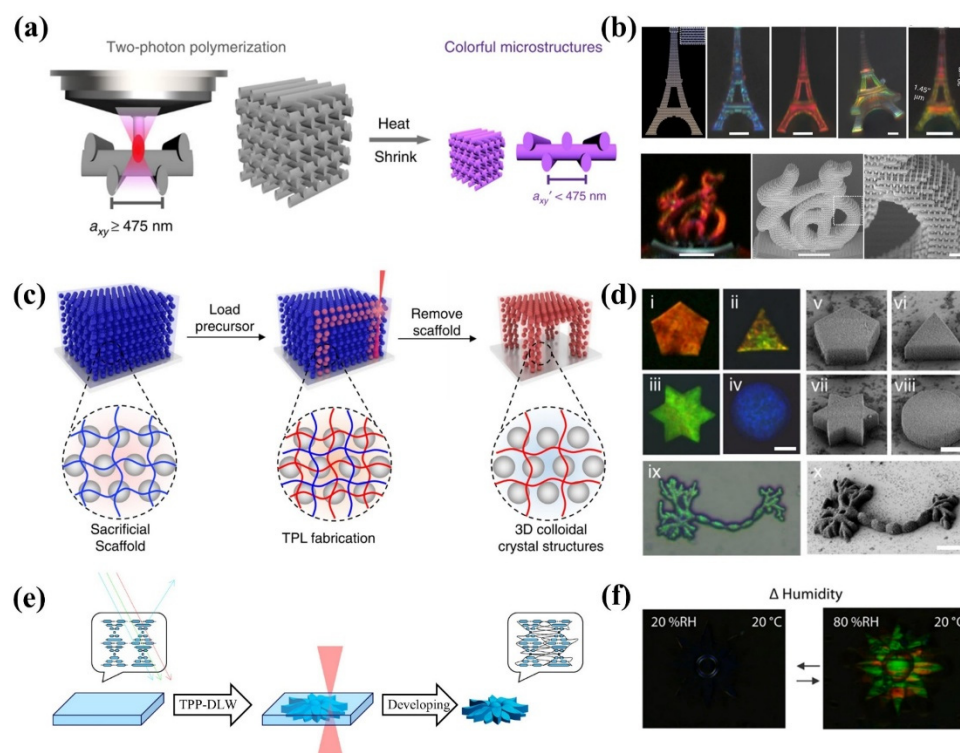


Figure 11. Structural-color materials via TPL. (a) Schematic of 3D-printed structural-color materials via heat-induced shrinking. (b) 3D color prints. Scale bars: 10 μm . Reproduced with permission [125]. Copyright 2019, Nature Publishing Group. (c) Schematic of the sacrificial-scaffold-mediated TPL process. (d) Colloidal crystal microstructures manufactured via the sacrificial-scaffold-mediated TPL. Scale bars: 20 μm . Reproduced with permission [126]. Copyright 2022, Nature Publishing Group. (e) Fabrication of 4D photonic microactuators via TPL. (f) Polarized optical micrographs of the flower presenting the color changes driven by humidity. Reproduced with permission [127]. Copyright 2020, American Chemical Society.

Endowing structural-color materials with highly precise 3D microarchitectures will open exciting prospects for novel applications. Liu et al. reported a sacrificial scaffold-mediated TPL method to enable the preparation of intricate 3D colloidal crystal microstructures possessing ordered nanoparticles inside (Figure 11c,d) [126]. Utilizing a degradable hydrogel scaffold, the disturbance effect of the femtosecond laser on the self-assembly of

nanoparticles can be solved. Thus, colloidal crystal microstructures in hydrogel and solid state with variable structural colors, free-designed geometries, and diverse compositions can be facily manufactured.

Stimuli-responsive photoresists can also be used to construct four-dimensional (4D) microstructures. Pozo et al. reported a photonic photoresist on a basis of supramolecular CLC was developed for fabricating stimuli-responsive photonic microactuators using two-photon polymerization direct laser writing, during which hydrogen bonds as supramolecular cross-linkers formed and cleaved after base treatment. This reversible process contributed to a stimuli responsive network (Figure 11e,f) [127]. Photonic 4D microactuators, including butterflies, flowers, and pillars with submicron resolution, have been created according to the advanced method. In addition, these structures exhibited dual responses to changes in humidity (directly) and temperature (indirectly). The hygroscopic character of the polymer network induced a shape change of up to 42% at 75% RH. The controlled expansion of the microactuators under conditions of various humidity and temperatures generates a corresponding color change for the adjustment of the nanoscale CLC pitch within the ordered network. This dual-mode responsive material can construct microrobots, which can release drugs and operate tissue repair within the physical environment in a directional manner.

5.3. Fused Deposition Modeling (FDM)

A FDM machine comprises a movable platform and a mechanical arm that controls the extrusion nozzle. Customized 3D structures can be created by controlling the movements of the nozzle and platform in the X, Y, and Z directions. The main difference between the FDM and DIW is the printing material. In DIW, the printing materials are in a liquid or paste state that can be directly extruded. In contrast, FDM requires the material to melt into filaments before printing. Similar to the previously mentioned DIW, FDM can also print structurally colored materials by incorporating suitable “building blocks” into the extruded material [128]. FDM enables to facilitate the practical applications including new passive color mixing [129], biocompatible scaffold [130] and biomimetic soft robots [131].

Boyle et al. designed a structural-colored material using a ring-opening polymerization method and used it as a building block in FDM to create 3D objects exhibiting structural color [132]. As depicted in Figure 12a, such a material is composed of dendritic BCPs that can self-assemble into various kinds of 1D, 2D, and 3D periodic structures. More specifically, BCPs can self-assemble into a layered structure with a scale similar to the wavelength of light, thus resulting in a structural color. By directly controlling the molecular weight of the block copolymers, the domain size of the nanostructure in the printed parts could be adjusted to tune the reflection peak across the visible light spectrum. Therefore, printed objects with diverse structural colors can be manufactured by altering the molecular weights of the BCPs (Figure 12b). This FDW 3D printing approach has the advantages of ease of use, reliability, and low cost; however, each object is merely available in an individual color. Thus, intricate parts of diffractive optical elements with customized optical properties can be fabricated without any pigments or dyes. The printed photonic objects with high precision enable to manipulate the wavefront in line with different wavelengths and generate the desired pattern or structural beams for filtering light or even guiding specified light frequencies around a curved geometry.

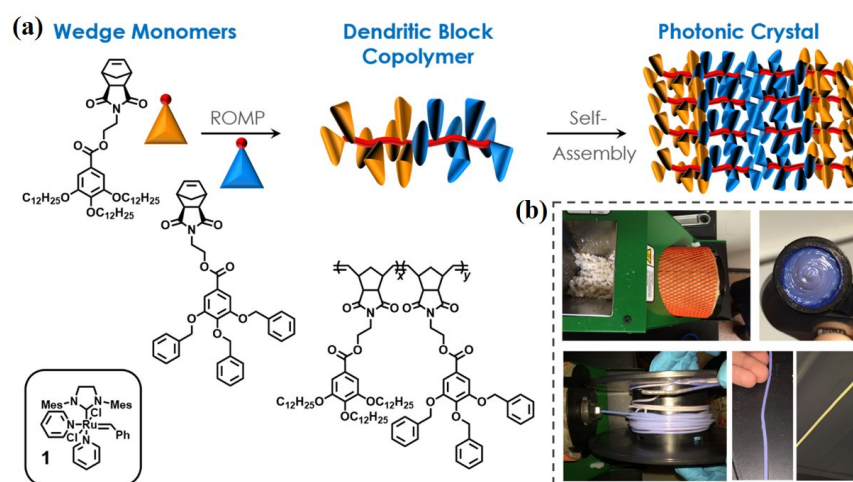


Figure 12. Structural-color materials via FDM. (a) Synthesis of the rigid-rod dendritic block copolymers and their self-assembly process. (b) Colorless block copolymers self-assemble into a colored filament during extrusion in the extruder nozzle. Reproduced with permission [132]. Copyright 2017, American Chemical Society.

Similar to DIW, FDM presents challenges such as surface roughness, restricted printing resolution, and limited material selection, as it also involves the controlled extrusion of certain materials from a nozzle. Moreover, to ensure the homogeneous dispersion of the nanoscale building blocks in the raw materials, a prolonged agitation and blending process is required, which is essential for achieving consistent color and optical properties throughout the printed objects. However, these extended processes require long-term stirring at high temperatures, which inhibits the incorporation of molecules with low thermal stability, such as bioactive molecules, into the raw materials.

6. Conclusions

In this work, we deliver a state-of-the-art review of the additive manufacturing of structural-color materials. A comprehensive overview of each manufacturing method, printable ink, properties, and limitations is presented in Table 1. For the DIW of structural-color materials, several printable inks, such as colloidal crystal inks, CLC inks, CNC inks, and BCP inks, have been formulated with both macroscopic printing rheology and microscopic self-assembly properties. For inkjet printing of structural-color materials, four strategies have been showcased: inkjet printing of colloidal crystals, inkjet printing of cellulose nanocrystals, inkjet printing inks on photonic polymer coatings, and inkjet printing based on total internal reflections. For the DLP of structural-color materials, the printable inks are cured from the liquid state to the solid state when exposed to UV or blue light; this process is repeated layer-by-layer until the entire 3D object has been constructed. For TPL of structural-color materials, high-energy pulse lasers are utilized to induce localized photochemical reactions within the material and produce high-resolution photonic nanostructures. In the FDM of structural-color materials, the printable build blocks self-assemble into filaments, and 3D structural-color objects are formed via filament extrusion.

Despite significant progress, additive manufacturing of structural-color materials for practical applications is still in the early phases of development. There are numerous challenges and opportunities to accelerate the development of this exciting field. On the one hand, the structural designability of additive manufacturing approaches is limited. Extrusion-based printing methods, like DIW, inkjet printing, and FDM, are characterized by rough surfaces and limited ink options because the printing materials and resolution are strictly constrained by the extrusion process. Structurally colored materials generated using DLP methods also exhibit notable layered structures and have limited design freedom. TPL can achieve high printing resolutions but faces challenges in efficiently printing large-scale structures. Therefore, novel additive manufacturing strategies that facilitate rapid and efficient material processing on a large scale are necessary to address these issues [133,134]. On the other hand, the capabilities of structure-color materials need to reinforce and extend its practical applications. The following key respects of printed structure-color materials should be considered to achieve this goal: (1) Printable structural-color inks: currently, the printable structural-color inks mainly involve colloidal particles, CLCs, CNCs, and BCPs. The limited material selection is a prevalent barrier for additive manufacturing manners, considering the compatibility of ink properties with additive manufacturing methods. Structural-color inks with high printability and stable periodic arrangements are urgently desired. Under the support of machine learning, the relevant abundant samples can be assembled and managed to predict ink formulations that optimize printability and color vibrancy. (2) High quality structural color: the color quality is often unsatisfied owing to the inevitable impact of the additive manufacturing process on the self-assembly. Considerable efforts are still required to obtain fine color resolution, broad color gamut, high color reflectivity, and improved color stability. Achieving this goal entails novel materials and self-assembly mechanism that can mitigate the undesired influence caused by the printing process [135]. Specifically, it can be solved via leveraging microfluidic droplet-based methods to precisely deposit self-assembling colloidal particles in a controlled manner either or applying programmable electric, magnetic, or acoustic fields to guide nanoparticles positioning for defect-free photonic structures. (3) Functionality: the long-term development goal of structure-color materials is to reinforce its functionality for practical applications. Key solutions for achieving this goal include using functional inks [136], printing combinatorial materials [137], and expansion of functional substrates capable of supporting structural colors [138,139], such as flexible substrates, textiles, and three-dimensional objects. The functionalization of materials with versatile and robust properties should be highlighted in the future, which aims at reinforcing resistance to environmental factors and exploiting extensive opportunities of environmentally conscious manufacturing practices. In the last decade, the additive manufacturing of structural-color materials has shown a feasible path for programming and manipulating photonic crystal objects in customized geometries. With the development of additive manufacturing technology and a deepening understanding of artificial structural-color materials, we believe that structural colors with free-designed structures and unprecedented properties will be developed in the near future. It is anticipated that the exploitation of additive manufacturing of bioinspired structural-color materials would yield vast opportunities and significant challenges, and joint collaboration from scientific researchers in the fields of multi-disciplinary specialties will expedite the

development of advanced manufacturing techniques, which mainly contains portable medical devices [140,141], biomedical imaging [142,143], personal wearable devices [144,145], etc.

Table 1. The manufacturing methods, printable inks, properties and limitations of structural colors.

Manufacturing Methods	Refs.	Printable Inks	Properties	Limitations
DIW	[71]	Silica particles/carbon black nanoparticles in acrylate resin	Customized structural-color graphics (absolute reflectivity > 80%)	High viscosity (>1.6 × 10 ⁶ mPa·s); Immiscibility of distinct inks for limited material selection
	[76]	CLC oligomer inks	Tunable chiroptical properties; Polarization independence of reflected light (−60° < θ < 60°)	Low saturation; Low pattern resolution
	[77]	CLC oligomer inks	Humidity-sensitive “hinge” driving actuation with reflected color shift	Low saturation Low pattern resolution
	[87]	CLC oligomer inks	Mechanochromic structural-color graphics; Sensitivity ≈1.64 nm% ^{−1}	Limited material selection
	[88]	HPC-gelatin-PACA inks	3D customized objects on arbitrary substrates; Environmental friendliness; Color tunability via temperature (from green to red in the range of 20–40 °C)	Low pattern resolution
	[89]	HPC-PEG inks	Optical response to mechanical deformation; Path-dependent tilt of the cholesteric domains	Low saturation; Low pattern resolution
	[90]	PDMS-b-PLA BBCP inks	Spatial patterning of structural colors; Exquisite modulation of microstructural (>70 nm)	Limited material selection; high cost
	[91]	PS-b-PLA cross-linkable BBCP inks	Multiple-color adjustment (from deep blue to orange via UV light irradiance from 411 to 0 μW/cm ²)	Limited material selection; high cost
	[100]	PS particles in mixture of deionized water and ethylene glycol with fluorescence	Angle independent structural colors; Enhanced brightness (>40 times); Wide viewing-angle (from 0° to 180°)	2D patterns only
	[101]	Silica nanoparticles in ATRP of PEG and DEX	Dual-color domes for nonuniform self-assembly	2D pattern only
[103]	PS nanoparticles in a binary solvent (ethylene glycol and formamide) with fluorescence	Unclonable multiplex encryption pattern; Rapid (≈2 s) and accurate (0 false alarm rate) authentication	2D pattern only	
Inkjet printing	[104]	Aqueous CNC suspension	Angle-dependent color and polarization-selective reflection; Ability to be printed in full-color dot-matrix patterns and bespoke images	2D pattern only
	[106]	colloidal quantum dots/CLC networks inks	Fluorescent LC polymer coatings; Full-color, high-resolution geminate patterns	Limited material selection
	[108]	BPLC inks	Erasable high-resolution “live” pattern	Limited material selection
	[110]	Fluorinated monomer in 1 wt% Pluronic F-127 in water	Full-color printing using only one transparent ink	Complex preparation process
DLP	[117]	NCPC composed of HENPs dispersed in a crosslinkable pre-gel solution	Tunable multicolor NCPC patterns and mechanical properties	Low Resolution; Rough surfaces;
	[118]	aqueous solution of PS latex particles mixing with CB, AM, PEGDA and TPO-H	Excellent shape fidelity; High precision; Angle dependence	Low Resolution; Rough surfaces;

Table 1. Cont.

Manufacturing Methods	Refs.	Printable Inks	Properties	Limitations
TPL	[125]	Silica polymeric woodpile microstructures	Multicolor microscopic 3D objects; The smallest achievable color voxel size: xy-directions: 1.45 μm z-direction: 2.63 μm	Limited size (μm level); Low efficiency
	[126]	Silica particles with hydrogel as sacrificial scaffold	Complex 3D colloidal crystal microstructures: minimum feature size down to 3 μm	Limited size; Low efficiency
	[127]	Supramolecular CLCs	Response to variations in humidity and temperature through modulation of their shape and color	Limited size; Low efficiency
FDM	[132]	Rigid-rod dendritic BCPs	Filter light or even guide specified light frequencies around a curved geometry	Low saturation; Low resolution

Author Contributions: L.W. and Y.Y. conceptualized the project. L.W. and W.F. supervised the project. Z.C. and Y.Y. drafted the manuscript and all authors contributed to revising it. All authors have read and agreed to the published version of manuscript.

Funding: The authors acknowledge the support from the Joint Fund for Regional Innovation and Development of National Natural Science Foundation China (No. U24A2078), the National Key R&D Program of China (2023YFB3812800), the National Natural Science Foundation of China (No. 52173181, 52203143 and 52327802), the Tianjin Science Fund for Distinguished Young Scholars (22JCJJC00060), Young Elite Scientists Sponsorship Program by CAST (No. 2022QNRC001).

Data Availability Statement: The data that support the findings of this study are available from the corresponding authors upon reasonable request.

Conflicts of Interest: The authors declare no conflict of financial interest.

References

- Cai, Z.; Li, Z.; Ravaine, S.; He, M.; Song, Y.; Yin, Y.; Zheng, H.; Teng, J.; Zhang, A. From colloidal particles to photonic crystals: Advances in self-assembly and their emerging applications. *Chem. Soc. Rev.* **2021**, *50*, 5898–5951. <https://doi.org/10.1039/D0CS00706D>.
- Foelen, Y.; Schenning, A.P.H.J. Optical indicators based on structural colored polymers. *Adv. Sci.* **2022**, *9*, 2200399. <https://doi.org/10.1002/advs.202200399>.
- Yang, J.; Zhang, X.; Zhang, X.; Wang, L.; Feng, W.; Li, Q. Beyond the visible: Bioinspired infrared adaptive materials. *Adv. Mater.* **2021**, *33*, 2004754. <https://doi.org/10.1002/adma.202004754>.
- Li, Z.; Fan, Q.; Yin, Y. Colloidal Self-Assembly Approaches to Smart Nanostructured Materials. *Chem. Rev.* **2022**, *122*, 4976–5067. <https://doi.org/10.1021/acs.chemrev.1c00482>.
- Xuan, Z.; Li, J.; Liu, Q.; Yi, F.; Wang, S.; Lu, W. Artificial Structural Colors and Applications. *Innovation* **2021**, *2*, 100081. <https://doi.org/10.1016/j.xinn.2021.100081>.
- Lopez-Garcia, M.; Masters, N.; O'Brien, H.E.; Lennon, J.; Atkinson, G.; Cryan, M.J.; Oulton, R.; Whitney, H.M. Light-induced dynamic structural color by intracellular 3D photonic crystals in brown algae. *Sci. Adv.* **2018**, *4*, eaan8917. <https://doi.org/10.1126/sciadv.aan8917>.
- Whitney, H.M.; Kolle, M.; Andrew, P.; Chittka, L.; Steiner, U.; Glover, B.J. Floral Iridescence, Produced by Diffractive Optics, Acts as a Cue for Animal Pollinators. *Science* **2009**, *323*, 130–133. <https://doi.org/10.1126/science.1166256>.
- Parker, A.R.; Welch, V.L.; Driver, D.; Martini, N. Opal analogue discovered in a weevil. *Nature* **2003**, *426*, 786–787. <https://doi.org/10.1038/426786a>.
- Teyssier, J.; Saenko, S.V.; van der Marel, D.; Milinkovitch, M.C. Photonic crystals cause active colour change in chameleons. *Nat. Commun.* **2015**, *6*, 6368. <https://doi.org/10.1038/ncomms7368>.
- Yoshioka, S.; Fujita, H.; Kinoshita, S.; Matsuhana, B. Alignment of crystal orientations of the multi-domain photonic crystals in *Parides sesostris* wing scales. *J. R. Soc. Interface* **2014**, *11*, 20131029. <https://doi.org/10.1098/rsif.2013.1029>.
- Saranathan, V.; Osuji, C.O.; Mochrie, S.; Noh, H.; Narayanan, S.; Sandy, A.; Dufresne, E.R.; Prum, R.O. Structure, function, and self-assembly of single network gyroid (I_4132) photonic crystals in butterfly wing scales. *Proc. Natl. Acad. Sci. USA* **2010**, *107*, 11676–11681. <https://doi.org/10.1073/pnas.0909616107>.
- Marlow, F.; Sharifi, P.; Brinkmann, R.; Mendive, C. Opals: Status and Prospects. *Angew. Chem. Int. Ed.* **2009**, *48*, 6212–6233. <https://doi.org/10.1002/anie.200900210>.
- Welch, V.; Lousse, V.; Deparis, O.; Parker, A.; Vigneron, J.P. Orange reflection from a three-dimensional photonic crystal in the scales of the weevil *Pachyrrhynchus congestus pavonius* (Curculionidae). *Phys. Rev. E* **2007**, *75*, 041919. <https://doi.org/10.1103/PhysRevE.75.041919>.

14. Sharma, V.; Crne, M.; Park, J.O.; Srinivasarao, M. Structural Origin of Circularly Polarized Iridescence in Jeweled Beetles. *Science* **2009**, *325*, 449–451. <https://doi.org/10.1126/science.1172051>.
15. Zhang, X.; Li, L.; Chen, Y.; Valenzuela, C.; Liu, Y.; Yang, Y.; Feng, Y.; Wang, L.; Feng, W. Mechanically Tunable Circularly Polarized Luminescence of Liquid Crystal-Templated Chiral Perovskite Quantum Dots. *Angew. Chem. Int. Ed.* **2024**, *63*, e202404202. <https://doi.org/10.1002/ange.202404202>.
16. Lin, X.; Shi, D.; Yi, G.; Yu, D. Structural color-based physical unclonable function. *Responsive Mater.* **2024**, *2*, e20230031. <https://doi.org/10.1002/rpm.20230031>.
17. Wang, F.; Lyu, R.; Xu, H.; Gong, R.; Ding, B. Tunable colors from responsive 2D materials. *Responsive Mater.* **2024**, *2*, e20240007. <https://doi.org/10.1002/rpm.20240007>.
18. Lyu, Q.; Li, M.; Zhang, L.; Zhu, J. Structurally-colored adhesives for sensitive, high-resolution, and non-invasive adhesion self-monitoring. *Nat. Commun.* **2024**, *15*, 8419. <https://doi.org/10.1038/s41467-024-52794-5>.
19. Li, H.; Zhao, G.; Zhu, M.; Guo, J.; Wang, C. Robust Large-Sized Photochromic Photonic Crystal Film for Smart Decoration and Anti-Counterfeiting. *ACS Appl. Mater. Interfaces* **2022**, *14*, 14618–14629. <https://doi.org/10.1021/acsami.2c01211>.
20. Fu, F.; Shang, L.; Chen, Z.; Yu, Y.; Zhao, Y. Bioinspired living structural color hydrogels. *Sci. Robot.* **2018**, *3*, eaar8580. <https://doi.org/10.1126/scirobotics.aar8580>.
21. Liu, C.; Fan, Z.; Tan, Y.; Fan, F.; Xu, H. Tunable Structural Color Patterns Based on the Visible-Light-Responsive Dynamic Diselenide Metathesis. *Adv. Mater.* **2020**, *32*, 1907569. <https://doi.org/10.1002/adma.201907569>.
22. Hong, W.; Yuan, Z.; Chen, X. Structural Color Materials for Optical Anticounterfeiting. *Small* **2020**, *16*, 1907626. <https://doi.org/10.1002/smll.201907626>.
23. Kim, I.; Jang, J.; Kim, G.; Lee, J.; Badloe, T.; Mun, J.; Rho, J. Pixelated bifunctional metasurface-driven dynamic vectorial holographic color prints for photonic security platform. *Nat. Commun.* **2021**, *12*, 3614. <https://doi.org/10.1038/s41467-021-23814-5>.
24. Zhu, C.; Jin, J.; Wang, Z.; Xu, Z.; Folgueras, M.C.; Jiang, Y.; Uzundal, C.B.; Le, H.K.D.; Wang, F.; Zheng, X.; et al. Supramolecular assembly of blue and green halide perovskites with near-unity photoluminescence. *Science* **2024**, *383*, 86–93. <https://doi.org/10.1126/science.adi4196>.
25. Yang, W.; Zheng, C.; Sun, L.; Bie, Z.; Yue, Y.; Li, X.; Sun, W.; Ikeda, T.; Wang, J.; Jiang, L. Spatiotemporal Programmability of 3D Chiral Color Units Driven by Ink Spontaneous Diffusion toward Customized Printing. *Adv. Mater.* **2024**, *36*, 2411988. <https://doi.org/10.1002/adma.202411988>.
26. Fang, Y.; Ni, Y.; Leo, S.-Y.; Taylor, C.; Basile, V.; Jiang, P. Reconfigurable photonic crystals enabled by pressure-responsive shape-memory polymers. *Nat. Commun.* **2015**, *6*, 7416. <https://doi.org/10.1038/ncomms8416>.
27. Lee, J.-S.; Je, K.; Kim, S.-H. Designing Multicolored Photonic Micropatterns through the Regioselective Thermal Compression of Inverse Opals. *Adv. Funct. Mater.* **2016**, *26*, 4587–4594. <https://doi.org/10.1002/adfm.201601095>.
28. Qin, L.; Gu, W.; Wei, J.; Yu, Y. Piecewise Phototuning of Self-Organized Helical Superstructures. *Adv. Mater.* **2018**, *30*, 1704941. <https://doi.org/10.1002/adma.201704941>.
29. Wang, Y.; Aurelio, D.; Li, W.; Tseng, P.; Zheng, Z.; Li, M.; Kaplan, D.L.; Liscidini, M.; Omenetto, F.G. Modulation of Multiscale 3D Lattices through Conformational Control: Painting Silk Inverse Opals with Water and Light. *Adv. Mater.* **2017**, *29*, 1702769. <https://doi.org/10.1002/adma.201702769>.
30. Truby, R.L.; Lewis, J.A. Printing soft matter in three dimensions. *Nature* **2016**, *540*, 371–378. <https://doi.org/10.1038/nature21003>.
31. del Pozo, M.; Sol, J.A.H.P.; Schenning, A.P.H.J.; Debije, M.G. 4D Printing of Liquid Crystals: What's Right for Me? *Adv. Mater.* **2021**, *33*, 2104390. <https://doi.org/10.1002/adma.202104390>.
32. Zhao, S.; Siqueira, G.; Drdova, S.; Norris, D.; Ubert, C.; Bonnin, A.; Galmarini, S.; Ganobjak, M.; Pan, Z.; Brunner, S.; et al. Additive manufacturing of silica aerogels. *Nature* **2020**, *584*, 387–392. <https://doi.org/10.1038/s41586-020-2594-0>.
33. Walker, D.A.; Hedrick, J.L.; Mirkin, C.A. Rapid, large-volume, thermally controlled 3D printing using a mobile liquid interface. *Science* **2019**, *366*, 360–364. <https://doi.org/10.1126/science.aax1562>.
34. Wang, L.; Dong, H.; Li, Y.; Liu, R.; Wang, Y.; Bisoyi, H.K.; Sun, L.; Yan, C.; Li, Q. Luminescence-driven reversible handedness inversion of self-organized helical superstructures enabled by a novel near-infrared light nanotransducer. *Adv. Mater.* **2015**, *27*, 2065–2069. <https://doi.org/10.1002/adma.201405690>.
35. Wang, L.; Dong, H.; Li, Y.; Xue, C.; Sun, L.; Yan, C.; Li, Q. Reversible Near-Infrared Light Directed Reflection in a Self-Organized Helical Superstructure Loaded with Upconversion Nanoparticles. *J. Am. Chem. Soc.* **2014**, *136*, 4480–4483. <https://doi.org/10.1021/ja500933h>.
36. Zeng, M.; King, D.; Huang, D.; Do, C.; Wang, L.; Chen, M.; Lei, S.; Lin, P.; Chen, Y.; Cheng, Z. Iridescence in nematics: Photonic liquid crystals of nanoplates in absence of long-range periodicity. *Proc. Natl. Acad. Sci. USA* **2019**, *116*, 18322–18327. <https://doi.org/10.1073/pnas.1906511116>.
37. Bauer, J.; Crook, C.; Baldacchini, T. A sinterless, low-temperature route to 3D print nanoscale optical-grade glass. *Science* **2023**, *380*, 960–966. <https://doi.org/10.1126/science.abq3037>.

38. Kuang, X.; Wu, J.; Chen, K.; Zhao, Z.; Ding, Z.; Hu, F.; Fang, D.; Qi, H.J. Grayscale digital light processing 3D printing for highly functionally graded materials. *Sci. Adv.* **2019**, *5*, eaav5790. <https://doi.org/10.1126/sciadv.aav5790>.
39. Hinton, T.J.; Jallerat, Q.; Palchesko, R.N.; Park, J.H.; Grodzicki, M.S.; Shue, H.-J.; Ramadan, M.H.; Hudson, A.R.; Feinberg, A.W. Three-dimensional printing of complex biological structures by freeform reversible embedding of suspended hydrogels. *Sci. Adv.* **2015**, *1*, e1500758. <https://doi.org/10.1126/sciadv.1500758>.
40. Yuk, H.; Lu, B.; Lin, S.; Qu, K.; Xu, J.; Luo, J.; Zhao, X. 3D printing of conducting polymers. *Nat. Commun.* **2020**, *11*, 1604. <https://doi.org/10.1038/s41467-020-15316-7>.
41. Kang, Y.; Zhao, J.; Zeng, Y.; Du, X.; Gu, Z. 3D Printing Photonic Crystals: A Review. *Small* **2024**, *20*, 2403525. <https://doi.org/10.1002/smll.202403525>.
42. Li, G.; Leng, M.; Wang, S.; Ke, Y.; Luo, W. Printable structural colors and their emerging applications. *Mater. Today* **2023**, *69*, 133–159. <https://doi.org/10.1016/j.mattod.2023.08.022>.
43. Zhao, C.; Wang, J.; Zhang, Z.; Chi, C. Research Progress on the Design of Structural Color Materials Based on 3D Printing. *Adv. Mater. Technol.* **2023**, *8*, 2200257. <https://doi.org/10.1002/admt.202200257>.
44. Withnall, R.; Silver, J.; Ireland, T.G.; Zhang, S.; Fern, G.R. Achieving structured colour in inorganic systems: Learning from the natural world. *Opt. Laser Technol.* **2011**, *43*, 401–409. <https://doi.org/10.1016/j.optlastec.2009.06.016>.
45. Meng, Z.; Wu, S.; Tang, B.; Ma, W.; Zhang, S. Structurally colored polymer films with narrow stop band, high angle-dependence and good mechanical robustness for trademark anti-counterfeiting. *Nanoscale* **2018**, *10*, 14755–14762. <https://doi.org/10.1039/C8NR04058C>.
46. Vignolini, S.; Rudall, P.J.; Rowland, A.V.; Reed, A.; Moyroud, E.; Faden, R.B.; Baumberg, J.J.; Glover, B.J.; Steiner, U. Pointillist structural color in *Pollia* fruit. *Proc. Natl. Acad. Sci. USA* **2012**, *109*, 15712–15715. <https://doi.org/10.1073/pnas.1210105109>.
47. Sharma, V.; Crne, V.; Park, J.O.; Srinivasarao, M. Bouligand Structures Underlie Circularly Polarized Iridescence of Scarab Beetles: A Closer View. *Mater. Today Proc.* **2014**, *1*, 161–171. <https://doi.org/10.1016/j.matpr.2014.09.019>.
48. Ma, J.; Yang, Y.; Valenzuela, C.; Zhang, X.; Wang, L.; Feng, W. Mechanochromic, Shape-Programmable and Self-Healable Cholesteric Liquid Crystal Elastomers Enabled by Dynamic Covalent Boronic Ester Bonds. *Angew. Chem. Int. Ed.* **2022**, *61*, e202116219. <https://doi.org/10.1002/anie.202116219>.
49. Liu, Y.; Ma, J.; Yang, Y.; Valenzuela, C.; Zhang, X.; Wang, L.; Feng, W. Smart chiral liquid crystal elastomers: Design, properties and application. *Smart Mol.* **2024**, *2*, e20230025. <https://doi.org/10.1002/smo.20230025>.
50. Li, X.; Yang, Y.; Valenzuela, C.; Zhang, X.; Xue, P.; Liu, Y.; Liu, C.; Wang, L. Mechanochromic and Conductive Chiral Nematic Nanostructured Film for Bioinspired Ionic Skins. *ACS Nano* **2023**, *17*, 12829–12841. <https://doi.org/10.1021/acsnano.3c04199>.
51. Yang, J.; Zhao, W.; He, W.; Yang, Z.; Wang, D.; Cao, H. Liquid crystalline blue phase materials with three-dimensional nanostructures. *J. Mater. Chem. C* **2019**, *7*, 13352–13366. <https://doi.org/10.1039/C9TC04380B>.
52. Yang, Y.; Wang, L.; Yang, H.; Li, Q. 3D Chiral Photonic Nanostructures Based on Blue-Phase Liquid Crystals. *Small Sci.* **2021**, *1*, 2100007. <https://doi.org/10.1002/smssc.202100007>.
53. Yang, J.; Zhao, W.; Yang, Z.; He, W.; Wang, J.; Ikeda, T.; Jiang, L. Photonic Shape Memory Polymer Based on Liquid Crystalline Blue Phase Films. *ACS Appl. Mater. Interfaces* **2019**, *11*, 46124–46131. <https://doi.org/10.1021/acsmi.9b14202>.
54. Valenzuela, C.; Ma, S.; Yang, Y.; Chen, Y.; Zhang, X.; Wang, L.; Feng, W. Direct Ink Writing of 3D Chiral Soft Photonic Crystals. *Adv. Funct. Mater.* **2025**, 2421280. <https://doi.org/10.1002/adfm.202421280>.
55. Sun, C.; Zhu, D.; Jia, H.; Yang, C.; Zheng, Z.; Wang, X. Bio-based visual optical pressure-responsive sensor. *Carbohydr. Polym.* **2021**, *260*, 117823. <https://doi.org/10.1016/j.carbpol.2021.117823>.
56. Chung, K.; Yu, S.; Heo, C.-J.; Shim, J.W.; Yang, S.-M.; Han, M.G.; Lee, H.-S.; Jin, Y.; Lee, S.Y.; Park, N.; et al. Flexible, Angle-Independent, Structural Color Reflectors Inspired by Morpho Butterfly Wings. *Adv. Mater.* **2012**, *24*, 2375–2379. <https://doi.org/10.1002/adma.201200521>.
57. Sveinbjörnsson, B.R.; Weitekamp, R.A.; Miyake, G.M.; Xia, Y.; Atwater, H.A.; Grubbs, R.H. Rapid self-assembly of brush block copolymers to photonic crystals. *Proc. Natl. Acad. Sci. USA* **2012**, *109*, 14332–14336. <https://doi.org/10.1073/pnas.1213055109>.
58. Guo, T.; Yu, X.; Zhao, Y.; Yuan, X.; Li, J.; Ren, L. Structure Memory Photonic Crystals Prepared by Hierarchical Self-Assembly of Semicrystalline Bottlebrush Block Copolymers. *Macromolecules* **2020**, *53*, 3602–3610. <https://doi.org/10.1021/acs.macromol.0c00274>.
59. Verduzco, R.; Li, X.; Pesek, S.L.; Stein, G.E. Structure, function, self-assembly, and applications of bottlebrush copolymers. *Chem. Soc. Rev.* **2015**, *44*, 2405–2420. <https://doi.org/10.1039/C4CS00329B>.
60. Dalsin, S.J.; Rions-Maehren, T.G.; Beam, M.D.; Bates, F.S.; Hillmyer, M.A.; Matsen, M.W. Bottlebrush Block Polymers: Quantitative Theory and Experiments. *ACS Nano* **2015**, *9*, 12233–12245. <https://doi.org/10.1021/acsnano.5b05473>.
61. Liu, H.; Wang, H.; Wang, H.; Deng, J.; Ruan, Q.; Zhang, W.; Abdelraouf, O.A.M.; Ang, N.S.S.; Dong, Z.; Yang, J.K.W.; et al. High-Order Photonic Cavity Modes Enabled 3D Structural Colors. *ACS Nano* **2022**, *16*, 8244–8252.

- <https://doi.org/10.1021/acsnano.2c01999>.
62. Yadav, A.; Yadav, N.; Agrawal, V.; Polyutov, S.P.; Tsipotan, A.S.; Karpov, S.V.; Slabko, V.V.; Yadav, V.S.; Wu, Y.; Zheng, H.; et al. State-of-art plasmonic photonic crystals based on self-assembled nanostructures. *J. Mater. Chem. C* **2021**, 9, 3368–3383. <https://doi.org/10.1039/D0TC05254J>.
 63. Kim, J.B.; Lee, H.-Y.; Chae, C.; Lee, S.Y.; Kim, S.-H. Advanced Additive Manufacturing of Structurally-Colored Architectures. *Adv. Mater.* **2024**, 36, 2307917. <https://doi.org/10.1002/adma.202307917>.
 64. Hou, X.; Li, F.; Song, Y.; Li, M. Recent Progress in Responsive Structural Color. *J. Phys. Chem. Lett.* **2022**, 13, 2885–2900. <https://doi.org/10.1021/acs.jpcclett.1c04219>.
 65. Xing, Y.; Fei, X.; Ma, J. Ultra-Fast Fabrication of Mechanical-Water-Responsive Color-Changing Photonic Crystals Elastomers and 3D Complex Devices. *Small* **2024**, 20, 2405426. <https://doi.org/10.1002/smll.202405426>.
 66. Bellis, I.D.; Martella, D.; Parmeggiani, C.; Wiersma, D.S.; Nocentini, S. Temperature Tunable 4D Polymeric Photonic Crystals. *Adv. Funct. Mater.* **2023**, 33, 2213162. <https://doi.org/10.1002/adfm.202213162>.
 67. Wang, H.; Ruan, Q.; Wang, H.; Rezaei, S.D.; Lim, K.T.P.; Liu, H.; Zhang, W.; Trisno, J.; Chan, J.Y.E.; Yang, J.K.W. Full Color and Grayscale Painting with 3D Printed Low-Index Nanopillars. *Nano Lett.* **2021**, 21, 4721–4729. <https://doi.org/10.1021/acs.nanolett.1c00979>.
 68. Kim, J.B.; Nam, S.K.; Park, S.; Amstad, E.; Kim, S.-H. Void-Free Photonic Surfaces Created by Adaptive Dense Packing of Emulsion Droplets. *Chem. Mater.* **2023**, 35, 261–270. <https://doi.org/10.1021/acs.chemmater.2c03124>.
 69. Zhu, Y.; Tang, T.; Zhao, S.; Joralmon, D.; Poit, Z.; Ahire, B.; Keshav, S.; Raje, A.R.; Blair, J.; Zhang, Z.; et al. Recent advancements and applications in 3D printing of functional optics. *Addit. Manuf.* **2022**, 25, 102682. <https://doi.org/10.1016/j.addma.2022.102682>.
 70. Tan, A.T.L.; Beroz, J.; Kolle, M.; Hart, A.J. Direct-Write Freeform Colloidal Assembly. *Adv. Mater.* **2018**, 30, 1803620. <https://doi.org/10.1002/adma.201803620>.
 71. Kim, J.B.; Chae, C.; Han, S.H.; Lee, S.Y.; Kim, S.-H. Direct writing of customized structural-color graphics with colloidal photonic inks. *Sci. Adv.* **2021**, 7, eabj8780. <https://doi.org/10.1126/sciadv.abj8780>.
 72. Kim, J.H.; Kim, J.B.; Kim, S.-H. Structural Color Inks Containing Photonic Microbeads for Direct Writing. *ACS Appl. Mater. Interfaces* **2024**, 16, 21098–21108. <https://doi.org/10.1021/acsami.4c01224>.
 73. Geng, Y.; Kizhakidathazhath, R.; Lagerwall, J.P.F. Robust cholesteric liquid crystal elastomer fibres for mechanochromic textiles. *Nat. Mater.* **2022**, 21, 1441–1447. <https://doi.org/10.1038/s41563-022-01355-6>.
 74. Li, X.; Chen, Y.; Du, C.; Liao, X.; Yang, Y.; Feng, W. Direct Ink Writing of Cephalopod Skin-Like Core-Shell Fibers from Cholesteric Liquid Crystal Elastomers and Dyed Solutions. *Adv. Funct. Mater.* **2024**, 34, 2413965. <https://doi.org/10.1002/adfm.202413965>.
 75. Bi, R.; Li, X.; Ou, X.; Huang, J.; Huang, D.; Chen, G.; Sheng, Y.; Hong, W.; Wang, Y.; Hu, W.; et al. 3D-Printed Biomimetic Structural Colors. *Small* **2024**, 19, 2306646. <https://doi.org/10.1002/smll.202306646>.
 76. Sol, J.A.H.P.; Sentjens, H.; Yang, L.; Grossiord, N.; Schenning, A.P.H.J.; Debije, M.G. Anisotropic Iridescence and Polarization Patterns in a Direct Ink Written Chiral Photonic Polymer. *Adv. Mater.* **2021**, 33, 2103309. <https://doi.org/10.1002/adma.202103309>.
 77. Sol, J.A.H.P.; Smits, L.G.; Schenning, A.P.H.J.; Debije, M.G. Direct Ink Writing of 4D Structural Colors. *Adv. Funct. Mater.* **2022**, 32, 2201766. <https://doi.org/10.1002/adfm.202201766>.
 78. Choi, J.; Choi, Y.; Lee, J.-H.; Kim, M.C.; Park, S.; Hyun, K.; Lee, K.M.; Yoon, T.-H.; Ahn, S.-k. Direct-Ink-Written Cholesteric Liquid Crystal Elastomer with Programmable Mechanochromic Response. *Adv. Funct. Mater.* **2024**, 33, 2310658. <https://doi.org/10.1002/adfm.202310658>.
 79. Chen, Y.; Valenzuela, C.; Liu, Y.; Yang, X.; Yang, Y.; Zhang, X.; Ma, S.; Bi, R.; Wang, L.; Feng, W. Biomimetic artificial neuromuscular fiber bundles with built-in adaptive feedback. *Matter* **2025**, 8, 101904. <https://doi.org/10.1016/j.matt.2024.10.022>.
 80. Yang, X.; Valenzuela, C.; Zhang, X.; Chen, Y.; Yang, Y.; Wang, L.; Feng, W. Robust integration of polymerizable perovskite quantum dots with responsive polymers enables 4D-printed self-deployable information display. *Matter* **2023**, 6, 1278–1294. <https://doi.org/10.1016/j.matt.2023.02.003>.
 81. Xue, P.; Chen, Y.; Xu, Y.; Valenzuela, C.; Zhang, X.; Bisoyi, H.K.; Yang, X.; Wang, L.; Xu, X.; Li, Q. Bioinspired MXene-Based Soft Actuators Exhibiting Angle-Independent Structural Color. *Nano-Micro Letters* **2023**, 15, 1. <https://doi.org/10.1007/s40820-022-00977-4>.
 82. Guan, Z.; Wang, L.; Bae, J. Advances in 4D printing of liquid crystalline elastomers: Materials, techniques, and applications. *Mater. Horiz.* **2022**, 9, 1825–1849. <https://doi.org/10.1039/D2MH00232A>.
 83. Ma, S.; Xue, P.; Tang, Y.; Bi, R.; Xu, X.; Wang, L.; Li, Q. Responsive soft actuators with MXene nanomaterials. *Responsive Mater.* **2024**, 2, e20230026. <https://doi.org/10.1002/rpm.20230026>.
 84. Lu, W.; Wang, R.; Si, M.; Zhang, Y.; Wu, S.; Zhu, N.; Wang, W.; Chen, T. Synergistic fluorescent hydrogel actuators with selective spatial shape/color-changing behaviors via interfacial supramolecular assembly. *SmartMat* **2024**, 5, e1190.

- <https://doi.org/10.1002/smm2.1190>.
85. Ma, J.; Yang, Y.; Zhang, X.; Xue, P.; Valenzuela, C.; Liu, Y.; Wang, L.; Feng, W. Mechanochromic and ionic conductive cholesteric liquid crystal elastomers for biomechanical monitoring and human–machine interaction. *Mater. Horiz.* **2024**, *11*, 217–226. <https://doi.org/10.1039/D3MH01386C>.
 86. Lv, P.; Lu, X.; Wang, L.; Feng, W. Nanocellulose-Based Functional Materials: From Chiral Photonics to Soft Actuator and Energy Storage. *Adv. Funct. Mater.* **2021**, *31*, 2104991. <https://doi.org/10.1002/adfm.202104991>.
 87. Yang, Y.; Zhang, X.; Valenzuela, C.; Bi, R.; Chen, Y.; Liu, Y.; Zhang, C.; Li, W.; Wang, L.; Feng, W. High-throughput printing of customized structural-color graphics with circularly polarized reflection and mechanochromic response. *Matter* **2024**, *7*, 2091–2107. <https://doi.org/10.1016/j.matt.2024.03.011>.
 88. Zhang, Z.; Wang, C.; Wang, Q.; Zhao, Y.; Shang, L. Cholesteric cellulose liquid crystal ink for three-dimensional structural coloration. *Proc. Natl. Acad. Sci. USA* **2022**, *119*, e2204113119. <https://doi.org/10.1073/pnas.2204113119>.
 89. Georgea, K.; Esmacilia, M.; Wang, J.; Taheri-Qazvini, N.; Abbaspourrad, A.; Sadatia, M. 3D printing of responsive chiral photonic nanostructures. *Proc. Natl. Acad. Sci. USA* **2023**, *120*, e2220032120. <https://doi.org/10.1073/pnas.2220032120>.
 90. Patel, B.B.; Walsh, D.J.; Kim, D.H.; Kwok, J.; Lee, B.; Guironnet, D.; Diao, Y. Tunable structural color of bottlebrush block copolymers through direct-write 3D printing from solution. *Sci. Adv.* **2020**, *6*, eaaz7202. <https://doi.org/10.1126/sciadv.aaz7202>.
 91. Jeona, S.; Kamble, Y.L.; Kang, H.; Shi, J.; Wade, M.A.; Patel, B.B.; Pan, T.; Rogers, S.A.; Sing, C.E.; Guironnet, D.; et al. Direct-ink-write cross-linkable bottlebrush block copolymers for on-the-fly control of structural color. *Proc. Natl. Acad. Sci. USA* **2024**, *121*, e2313617121. <https://doi.org/10.1073/pnas.2313617121>.
 92. Shanker, R.; Sardar, S.; Chen, S.; Gamage, S.; Rossi, S.; Jonsson, M.P. Noniridescent Biomimetic Photonic Microdomes by Inkjet Printing. *Nano Lett.* **2020**, *20*, 7243–7250. <https://doi.org/10.1021/acs.nanolett.0c02604>.
 93. Hu, Z.; Bradshaw, N.P.; Vanthournout, B.; Forman, C.; Gnanasekaran, K.; Thompson, M.P.; Smeets, P.; Dhinojwala, A.; Shawkey, M.D.; Hersam, M.C.; et al. Non-Iridescent Structural Color Control via Inkjet Printing of Self-Assembled Synthetic Melanin Nanoparticles. *Chem. Mater.* **2021**, *33*, 6433–6442. <https://doi.org/10.1021/acs.chemmater.1c01719>.
 94. Bai, L.; Xie, Z.; Wang, W.; Yuan, C.; Zhao, Y.; Mu, Z.; Zhong, Q.; Gu, Z. Bio-Inspired Vapor-Responsive Colloidal Photonic Crystal Patterns by Inkjet Printing. *ACS Nano* **2014**, *8*, 11094–11100. <https://doi.org/10.1021/nn504659p>.
 95. Li, W.; Wang, Y.; Li, M.; Garbarini, L.P.; Omenetto, F.G. Inkjet Printing of Patterned, Multispectral, and Biocompatible Photonic Crystals. *Adv. Mater.* **2019**, *31*, 1901036. <https://doi.org/10.1002/adma.201901036>.
 96. Moirangthem, M.; Schenning, A.P.H.J. Full Color Camouflage in a Printable Photonic Blue-Colored Polymer. *ACS Appl. Mater. Interfaces* **2018**, *10*, 4168–4172. <https://doi.org/10.1021/acsami.7b17892>.
 97. Kuang, M.; Wang, L.; Song, Y. Controllable Printing Droplets for High-Resolution Patterns. *Adv. Mater.* **2014**, *26*, 6950–6958. <https://doi.org/10.1002/adma.201305416>.
 98. Liu, M.; Wang, J.; He, M.; Wang, L.; Li, F.; Jiang, L.; Song, Y. Inkjet Printing Controllable Footprint Lines by Regulating the Dynamic Wettability of Coalescing Ink Droplets. *ACS Appl. Mater. Interfaces* **2014**, *6*, 13344–13348. <https://doi.org/10.1021/am5042548>.
 99. Wu, L.; Dong, Z.; Kuang, M.; Li, Y.; Li, F.; Jiang, L.; Song, Y. Printing Patterned Fine 3D Structures by Manipulating the Three Phase Contact Line. *Adv. Funct. Mater.* **2015**, *25*, 2237–2242. <https://doi.org/10.1002/adfm.201404559>.
 100. Kuang, M.; Wang, J.; Bao, B.; Li, F.; Wang, L.; Jiang, L.; Song, Y. Inkjet Printing Patterned Photonic Crystal Domes for Wide Viewing-Angle Displays by Controlling the Sliding Three Phase Contact Line. *Adv. Opt. Mater.* **2014**, *2*, 34–38. <https://doi.org/10.1002/adom.201300369>.
 101. Li, C.; Yu, Y.; Li, H.; Tian, J.; Guo, W.; Shen, Y.; Cui, H.; Pan, Y.; Song, Y.; Shum, H.C. One-Pot Self-Assembly of Dual-Color Domes Using Mono-Sized Silica Nanoparticles. *Nano Lett.* **2022**, *22*, 5236–5243. <https://doi.org/10.1021/acs.nanolett.2c01090>.
 102. Li, C.; Yu, Y.; Li, H.; Lin, H.; Cui, H.; Pan, Y.; Zhang, R.; Song, Y.; Shum, H.C. Heterogeneous Self-Assembly of a Single Type of Nanoparticle Modulated by Skin Formation. *ACS Nano* **2023**, *17*, 11645–11654. <https://doi.org/10.1021/acsnano.3c02082>.
 103. Gao, Y.; Ge, K.; Zhang, Z.; Li, Z.; Hu, S.; Ji, H.; Li, M.; Feng, H. Fine Optimization of Colloidal Photonic Crystal Structural Color for Physically Unclonable Multiplex Encryption and Anti-Counterfeiting. *Adv. Sci.* **2024**, *11*, 2305876. <https://doi.org/10.1002/advs.202305876>.
 104. Williams, C.A.; Parker, R.M.; Kyriacou, A.; Murace, M.; Vignolini, S. Inkjet Printed Photonic Cellulose Nanocrystal Patterns. *Adv. Mater.* **2024**, *36*, 2307563. <https://doi.org/10.1002/adma.202307563>.
 105. Moirangthem, M.; Scheers, A.F.; Schenning, A.P.H.J. A full color photonic polymer, rewritable with a liquid crystal ink. *Chem. Commun.* **2018**, *54*, 4425–4428. <https://doi.org/10.1039/C8CC02188K>.
 106. Liu, X.; Cui, S.; Qin, L.; Yu, Y. Two-Chromatic Printing Creates Skin-Inspired Geminate Patterns Featuring Crosstalk-Free Chemical and Physical Colors. *Adv. Opt. Mater.* **2024**, *12*, 2302573. <https://doi.org/10.1002/adom.202302573>.
 107. Yang, J.; Zhao, W.; Yang, Z.; He, W.; Wang, J.; Ikeda, T.; Jiang, L. Printable photonic polymer coating based on a

- monodomain blue phase liquid crystal network. *J. Mater. Chem. C* **2019**, *7*, 13764–13769. <https://doi.org/10.1039/C9TC05052C>.
108. Meng, F.; Zheng, C.; Yang, W.; Guan, B.; Wang, J.; Ikeda, T.; Jiang, L. High-Resolution Erasable “Live” Patterns Based on Controllable Ink Diffusion on the 3D Blue-Phase Liquid Crystal Networks. *Adv. Funct. Mater.* **2022**, *32*, 2110985. <https://doi.org/10.1002/adfm.202110985>.
109. Yang, Y.; Zhang, X.; Chen, Y.; Yang, X.; Ma, J.; Wang, J.; Wang, L.; Feng, W. Bioinspired Color-Changing Photonic Polymer Coatings Based on Three-Dimensional Blue Phase Liquid Crystal Networks. *ACS Appl. Mater. Interfaces* **2021**, *13*, 41102–41111. <https://doi.org/10.1021/acsami.1c11711>.
110. Goodling, A.E.; Nagelberg, S.; Kaehr, B.; Meredith, C.H.; Cheon, S.I.; Saunders, A.P.; Kolle, M.; Zarzar, L.D. Colouration by total internal reflection and interference at microscale concave interfaces. *Nature* **2019**, *566*, 523–527. <https://doi.org/10.1038/s41586-019-0946-4>.
111. Wang, L.; Urbas, A.M.; Li, Q. Nature-Inspired Emerging Chiral Liquid Crystal Nanostructures: From Molecular Self-Assembly to DNA Mesophase and Nanocolloids. *Adv. Mater.* **2020**, *32*, 1801335. <https://doi.org/10.1002/adma.201801335>.
112. Zhang, X.; Xu, Y.; Valenzuela, C.; Zhang, X.; Wang, L.; Feng, W.; Li, Q. Liquid crystal-templated chiral nanomaterials: From chiral plasmonics to circularly polarized luminescence. *Light Sci. Appl.* **2022**, *11*, 223. <https://doi.org/10.1038/s41377-022-00913-6>.
113. Yang, Y.; Liu, Y.; Chen, Y.; Wang, L.; Feng, W. Bioinspired Stretchable Polymers for Dynamic Optical and Thermal Regulation. *Adv. Energy Sustain. Res.* **2024**, *5*, 2300289. <https://doi.org/10.1002/aesr.202300289>.
114. Li, K.; Li, T.; Zhang, T.; Li, H.; Li, A.; Li, Z.; Lai, X.; Hou, X.; Wang, Y.; Shi, L.; et al. Facile full-color printing with a single transparent ink. *Sci. Adv.* **2021**, *7*, eabh1992. <https://doi.org/10.1126/sciadv.abh1992>.
115. Zhang, Y.; Dong, Z.; Li, C.; Du, H.; Fang, N.X.; Wu, L.; Song, Y. Continuous 3D printing from one single droplet. *Nat. Commun.* **2020**, *11*, 4685. <https://doi.org/10.1038/s41467-020-18518-1>.
116. Llorens, J.S.; Barbera, L.; Demirörs, A.F.; Studar, A.R. Light-Based 3D Printing of Complex-Shaped Photonic Colloidal Glasses. *Adv. Mater.* **2023**, *35*, 2302868. <https://doi.org/10.1002/adma.202302868>.
117. Liao, J.; Ye, C.; Guo, J.; Garciamendez-Mijares, C.E.; Agrawal, P.; Kuang, X.; Japo, J.O.; Wang, Z.; Mu, X.; Li, W.; et al. 3D-printable colloidal photonic crystals. *Mater. Today* **2022**, *56*, 29–41. <https://doi.org/10.1016/j.mattod.2022.02.014>.
118. Zhang, Y.; Zhang, L.; Zhang, C.; Wang, J.; Liu, J.; Ye, C.; Dong, Z.; Wu, L.; Song, Y. Continuous resin refilling and hydrogen bond synergistically assisted 3D structural color printing. *Nat. Commun.* **2022**, *13*, 7095. <https://doi.org/10.1038/s41467-022-34866-6>.
119. Zhang, X.; Yang, Y.; Xue, P.; Valenzuela, C.; Chen, Y.; Yang, X.; Wang, L.; Feng, W. Three-Dimensional Electrochromic Soft Photonic Crystals Based on MXene-Integrated Blue Phase Liquid Crystals for Bioinspired Visible and Infrared Camouflage. *Angew. Chem. Int. Ed.* **2022**, *61*, e202211030. <https://doi.org/10.1002/anie.202211030>.
120. Yang, H.; Fang, H.; Wang, C.; Wang, Y.; Qi, C.; Zhang, Y.; Zhou, Q.; Huang, M.; Wang, M.; Wu, M. 3D printing of customized functional devices for smart biomedical systems. *SmartMat* **2024**, *5*, e1244. <https://doi.org/10.1002/smm2.1244>.
121. Hou, I.C.-Y.; Li, L.; Zhang, H.; Naumov, P. Smart molecular crystal switches. *Smart Mol.* **2024**, *2*, e20230031. <https://doi.org/10.1002/smo.20230031>.
122. Qi, Y.; Zhang, S. Recent progress in low-swellable polymer-based smart photonic crystal sensors. *Smart Mol.* **2023**, *1*, e20230018. <https://doi.org/10.1002/smo.20230018>.
123. Liu, Y.; Bi, R.; Zhang, X.; Chen, Y.; Valenzuela, C.; Yang, Y.; Liu, H.; Yang, L.; Wang, L.; Feng, W. Cephalopod-Inspired MXene-Integrated Mechanochromic Cholesteric Liquid Crystal Elastomers for Visible-Infrared-Radar Multispectral Camouflage. *Angew. Chem. Int. Ed.* **2024**, *137*, e202422636. <https://doi.org/10.1002/ange.202422636>.
124. Wang, H.; Zhang, W.; Ladika, D.; Yu, H.; Gailevičius, D.; Wang, H.; Pan, C.-F.; Nair, P.N.S.; Ke, Y.; Mori, T.; et al. Two-Photon Polymerization Lithography for Optics and Photonics: Fundamentals, Materials, Technologies, and Applications. *Adv. Funct. Mater.* **2023**, *33*, 2214211. <https://doi.org/10.1002/adfm.202214211>.
125. Liu, Y.; Wang, H.; Ho, J.; Ng, R.C.; Ng, R.J.H.; Hall-Chen, V.H.; Koay, E.H.H.; Dong, Z.; Liu, H.; Qiu, C.-W.; et al. Structural color three-dimensional printing by shrinking photonic crystals. *Nat. Commun.* **2019**, *10*, 4340. <https://doi.org/10.1038/s41467-019-12360-w>.
126. Liu, K.; Ding, H.; Li, S.; Niu, Y.; Zeng, Y.; Zhang, J.; Du, X.; Gu, Z. 3D printing colloidal crystal microstructures via sacrificial-scaffold-mediated two-photon lithography. *Nat. Commun.* **2022**, *13*, 4563. <https://doi.org/10.1038/s41467-022-32317-w>.
127. del Pozo, M.; Delaney, C.; Bastiaansen, C.W.M.; Diamond, D.; Schenning, A.P.H.J.; Florea, L. Direct Laser Writing of Four-Dimensional Structural Color Microactuators Using a Photonic Photoresist. *ACS Nano* **2020**, *14*, 9832–9839. <https://doi.org/10.1021/acsnano.0c02481>.
128. Cano-Vicent, A.; Tambuwala, M.M.; Hassan, S.S.; Barh, D.; Aljabali, A.A.A.; Birkett, M.; Arjunan, A.; Serrano-Aroca, A. Fused deposition modelling: Current status, methodology, applications and future prospects. *Addit. Manuf.* **2021**, *47*, 102378. <https://doi.org/10.1016/j.addma.2021.102378>.

129. Reiner, T.; Carr, N.; Měch, R.; Št'ava, O.; Dachsbacher, C.; Miller, G. Dual-color mixing for fused deposition modeling printers. *Com. Gra. For.* **2014**, *33*, 479–486. <https://doi.org/10.1111/cgf.12319>.
130. Korpela, J.; Kokkari, A.; Korhonen, H.; Malin, M.; Närhi, T.; Seppälä, J. Biodegradable and bioactive porous scaffold structures prepared using fused deposition modeling. *J Biomed. Mater. Res. Part B* **2013**, *101B*, 610–619. <https://doi.org/10.1002/jbm.b.32863>.
131. Wang, J.; Wang, Z.; Song, Z.; Ren, L.; Liu, Q.; Ren, L. Biomimetic Shape–Color Double-Responsive 4D Printing. *Adv. Mater. Technol.* **2019**, *4*, 1900293. <https://doi.org/10.1002/admt.201900293>.
132. Boyle, B.M.; French, T.A.; Pearson, R.M.; McCarthy, B.G.; Miyake, G.M. Structural Color for Additive Manufacturing: 3D-Printed Photonic Crystals from Block Copolymers. *ACS Nano* **2017**, *11*, 3052–3058. <https://doi.org/10.1021/acsnano.7b00032>.
133. Zhang, W.; Wang, H.; Wang, H.; Chan, J.Y.E.; Liu, H.; Zhang, B.; Zhang, Y.-F.; Agarwal, K.; Yang, X.; Ranganath, A.S.; et al. Structural multi-colour invisible inks with submicron 4D printing of shape memory polymers. *Nat. Commun.* **2021**, *12*, 112. <https://doi.org/10.1038/s41467-020-20300-2>.
134. Rorem, B.A.; Cho, T.H.; Farjam, N.; Lenef, J.D.; Barton, K.; Dasgupta, N.P.; Guo, L.J. Integrating Structural Colors with Additive Manufacturing Using Atomic Layer Deposition. *ACS Appl. Mater. Interfaces* **2022**, *14*, 31099–31108. <https://doi.org/10.1021/acsmi.2c05940>.
135. Xiao, X.; Chen, Z.-J.; Varley, R.J.; Li, C.-H. Smart bistable coordination complexes. *Smart Mol.* **2024**, *2*, e20230028. <https://doi.org/10.1002/smo.20230028>.
136. Demirörs, A.F.; Poloni, E.; Chiesa, M.; Bargardi, F.L.; Binelli, M.R.; Woigk, W.; de Castro, L.D.C.; Kleger, N.; Coulter, F.B.; Sicher, A.; et al. Three-dimensional printing of photonic colloidal glasses into objects with isotropic structural color. *Nat. Commun.* **2022**, *13*, 4397. <https://doi.org/10.1038/s41467-022-32060-2>.
137. Zeng, M.; Du, Y.; Jiang, Q.; Kempf, N.; Wei, C.; Bimrose, M.V.; Tanvir, A.N.M.; Xu, H.; Chen, J.; Kirsch, D.J.; et al. High-throughput printing of combinatorial materials from aerosols. *Nature* **2023**, *617*, 292–298. <https://doi.org/10.1038/s41586-023-05898-9>.
138. Bai, L.; Mai, V.C.; Lim, Y.; Hou, S.; Möhwald, H.; Duan, H. Large-Scale Noniridescent Structural Color Printing Enabled by Infiltration-Driven Nonequilibrium Colloidal Assembly. *Adv. Mater.* **2018**, *30*, 1705667. <https://doi.org/10.1002/adma.201705667>.
139. Jiang, H.; Kaminska, B. Scalable Inkjet-Based Structural Color Printing by Molding Transparent Gratings on Multilayer Nanostructured Surfaces. *ACS Nano* **2018**, *12*, 3112–3125. <https://doi.org/10.1021/acsnano.7b08580>.
140. Zhang, X.; Zhou, K.; Zhao, Z.; Lin, Y. Printable Photonic Materials and Devices for Smart Healthcare. *Adv. Mater.* **2025**, 2418729. <https://doi.org/10.1002/adma.202418729>.
141. Chen, H.; Bian, F.; Luo, Z.; Zhao, Y. Biomimetic Anticoagulated Porous Particles with Self-Reporting Structural Colors. *Adv. Sci.* **2024**, *11*, 2400189. <https://doi.org/10.1002/advs.202400189>.
142. Middleton, R.; Tunstad, S.A.; Knapp, A.; Winters, S.; McCallum, S.; Whitney, H. Self-assembled, disordered structural color from fruit wax bloom. *Sci. Adv.* **2024**, *10*, eadk4219. <https://doi.org/10.1126/sciadv.adk4219>.
143. Kang, X.; Du, Z.; Yang, S.; Liang, M.; Liu, Q.; Qi, J. Smart molecular probes with controllable photophysical property for smart medicine. *Smart Mol.* **2024**, *2*, e20240033. <https://doi.org/10.1002/smo.20240033>.
144. Kim, T.; Park, T.H.; Lee, J.W.; Lee, D.; Mun, S.; Kim, G.; Kim, Y.; Kim, G.; Park, J.W.; Lee, K.; et al. Self-Powered Sweat-Responsive Structural Color Display. *Adv. Funct. Mater.* **2024**, *34*, 2314721. <https://doi.org/10.1002/adfm.202314721>.
145. Liao, Z.-H.; Wang, F. Light-controlled smart materials: Supramolecular regulation and applications. *Smart Mol.* **2024**, *2*, e20240036. <https://doi.org/10.1002/smo.20240036>.